



Article

# The Genetic Dissection of Nitrogen Use-Related Traits in Flax (*Linum usitatissimum* L.) at the Seedling Stage through the Integration of Multi-Locus GWAS, RNA-seq and Genomic Selection

Braulio J. Soto-Cerda <sup>1,2,\*</sup>, Giovanni Larama <sup>3,4</sup> , Sylvie Cloutier <sup>5</sup> , Bourlaye Fofana <sup>6,\*</sup> , Claudio Inostroza-Blancheteau <sup>1,2</sup> and Gabriela Aravena <sup>1</sup>

- <sup>1</sup> Departamento de Ciencias Agropecuarias y Acuícolas, Universidad Católica de Temuco, Rudecindo Ortega 02950, Temuco 4781312, Chile; claudio.inostroza@uct.cl (C.I.-B.); gaby.aravena@gmail.com (G.A.)
- <sup>2</sup> Núcleo de Investigación en Producción Alimentaria, Facultad de Recursos Naturales, Universidad Católica de Temuco, Rudecindo Ortega 02950, Temuco 4781312, Chile
- <sup>3</sup> Center of Plant, Soil Interaction and Natural Resources Biotechnology, Scientific and Technological Bioresource Nucleus, Universidad de La Frontera, Temuco 4811230, Chile; giovanni.larama@ufrontera.cl
- <sup>4</sup> Biocontrol Research Laboratory, Universidad de La Frontera, Temuco 4811230, Chile
- <sup>5</sup> Ottawa Research and Development Centre, Agriculture and Agri-Food Canada, 960 Carling Avenue, Ottawa, ON K1A 0C6, Canada; sylviej.cloutier@agr.gc.ca
- <sup>6</sup> Charlottetown Research and Development Centre, Agriculture and Agri-Food Canada, 440 University Avenue, Charlottetown, PE C1A 4N6, Canada
- \* Correspondence: bsoto@uct.cl (B.J.S.-C.); bourlaye.fofana@agr.gc.ca (B.F.)



**Citation:** Soto-Cerda, B.J.; Larama, G.; Cloutier, S.; Fofana, B.; Inostroza-Blancheteau, C.; Aravena, G. The Genetic Dissection of Nitrogen Use-Related Traits in Flax (*Linum usitatissimum* L.) at the Seedling Stage through the Integration of Multi-Locus GWAS, RNA-seq and Genomic Selection. *Int. J. Mol. Sci.* **2023**, *24*, 17624. <https://doi.org/10.3390/ijms242417624>

Academic Editor: Michael Moustakas

Received: 3 November 2023

Revised: 10 December 2023

Accepted: 12 December 2023

Published: 18 December 2023



**Copyright:** © 2023 by the authors. Licensee MDPI, Basel, Switzerland. This article is an open access article distributed under the terms and conditions of the Creative Commons Attribution (CC BY) license (<https://creativecommons.org/licenses/by/4.0/>).

**Abstract:** Nitrogen (N), the most important macro-nutrient for plant growth and development, is a key factor that determines crop yield. Yet its excessive applications pollute the environment and are expensive. Hence, studying nitrogen use efficiency (NUE) in crops is fundamental for sustainable agriculture. Here, an association panel consisting of 123 flax accessions was evaluated for 21 NUE-related traits at the seedling stage under optimum N (N+) and N deficiency (N−) treatments to dissect the genetic architecture of NUE-related traits using a multi-omics approach integrating genome-wide association studies (GWAS), transcriptome analysis and genomic selection (GS). Root traits exhibited significant and positive correlations with NUE under N− conditions ( $r = 0.33$  to  $0.43$ ,  $p < 0.05$ ). A total of 359 QTLs were identified, accounting for 0.11% to 23.1% of the phenotypic variation in NUE-related traits. Transcriptomic analysis identified 1034 differentially expressed genes (DEGs) under contrasting N conditions. DEGs involved in N metabolism, root development, amino acid transport and catabolism and others, were found near the QTLs. GS models to predict NUE stress tolerance index (NUE\_STI) trait were tested using a random genome-wide SNP dataset and a GWAS-derived QTLs dataset. The latter produced superior prediction accuracy ( $r = 0.62$  to  $0.79$ ) compared to the genome-wide SNP marker dataset ( $r = 0.11$ ) for NUE\_STI. Our results provide insights into the QTL architecture of NUE-related traits, identify candidate genes for further studies, and propose genomic breeding tools to achieve superior NUE in flax under low N input.

**Keywords:** *Linum usitatissimum*; nitrogen use efficiency; GWAS; RNA-seq; genomic selection

## 1. Introduction

Nitrogen (N) is the most important mineral nutrient for plant growth and development, and it is key in determining yield in non-N-fixing crops [1]. In the last four decades, a twofold increase in food production was only achieved through a disproportionate sevenfold increase in the use of N fertilizer [2]. In 2018, 186 million tons of N fertilizer were utilized globally [3]. Given the world's projected human population by 2050, a further threefold increase in N input will be needed to fulfill the global food demand [4]. Although

N has the most direct impact on crop production, plants can only uptake and use 30–40% of the applied N [5]. The unused N, lost in the atmosphere and through groundwater and rivers, causes environmental pollution [5,6]. Moreover, chemical N production greatly depends on fossil energy, contributing to additional greenhouse emissions and raising fertilizer costs [7]. Generally, low N use efficiency (NUE) in crops leads to excessive use of N fertilizer, which is not environment-friendly or cost-effective for food production [3,5].

NUE is defined as crop yield per unit of available N in the soil [8] and consists of two main components: N uptake efficiency (NupE), which includes traits such as root architecture and transporter activity; and N utilization efficiency (NutE), which includes all the processes related to the plant's capacity to assimilate and remobilize N into the seeds [9,10]. It is of strategic importance to improve crops' NUE because a mere 1% increase in NUE would translate into ~\$2.3 B USD annual savings in N fertilizer costs, while also reducing the environmental footprint [11].

Plants uptake N from the soil mainly as nitrate ( $\text{NO}_3^-$ ), ammonium ( $\text{NH}_4^+$ ) or as amino acids under specific soil conditions [12,13]. A plant's response to N involves multiple genes that control root/shoot growth, N metabolism, and N content. In *Arabidopsis*, four families of nitrate transporters, *NRT1*, *NRT2*, *CLC* and *SLAC/SLAH*, have been characterized by Masclaux-Daubresse et al. [9]. Among the *NRT1* gene family, *NRT1.1* plays roles in  $\text{NO}_3^-$  uptake and translocation from roots to shoots [14]. In addition to *NRT1.1*, *NRT1.2* and *NAXT1* have also been reported to be involved in  $\text{NO}_3^-$  uptake with *NRT1.2* and *NAXT1* ensuring influx and efflux activities, respectively [15]. *NRT1.8*, *NRT1.5* and *NRT1.9* were described as major transporters for long-distance  $\text{NO}_3^-$  distribution. *NRT1.8* is known to modulate  $\text{NO}_3^-$  loading into the xylem parenchyma cells within the vascular system [16], whereas *NRT1.9* mediates  $\text{NO}_3^-$  loading into the root phloem, thereby influencing  $\text{NO}_3^-$  translocation and distribution [17]. *NRT1.11* and *NRT1.12* are expressed in mature leaves and mediate  $\text{NO}_3^-$  distribution to young tissues [18]. Once  $\text{NO}_3^-$  is absorbed by roots, it is first reduced to nitrite ( $\text{NO}_2^-$ ) by a cytosolic nitrate reductase (NR), and then to  $\text{NH}_4^+$  by a nitrite reductase (NiR) [19]. Together with glutamate synthase (GOGAT), glutamine synthetase (GS), a key enzyme in N assimilation and remobilization, forms the GS-GOGAT cycle in which inorganic  $\text{NH}_4^+$  is converted into glutamine [19]. In addition to the transport and assimilation genes, many transcription factors are involved in the regulation of NUE (reviewed by Masclaux-Daubresse [9]; Hudson [20]; Alvarez [21]; Luo [13]). The extensive nature of this gene network illustrates the complexity of N response, NUE regulation, and its underlying genetic mechanisms, making conventional plant breeding progress slow and success not guaranteed.

A variety of traits contributing to NUE in plants have been evaluated in many biparental populations and the associated QTL studies have been reported [22–24]. At the seedling stage, QTL studies have focused on NUE-related traits and their associations with root system architecture (RSA) traits. In maize, 184 NUE-related QTLs and 147 RSA-related QTLs were identified [10]. Similarly, five and six stable pleiotropic QTL influencing RSA-NUE traits were reported in rapeseed and wheat, respectively. In the adult plant stage, QTL studies have focused on yield-related traits, such as grain and biomass N content, physiological traits and their correlations to NupE and NutE [22,24,25]. In maize, Hirel [25] identified one QTL that collocated with NUE, yield, nitrate content, nitrate reductase and glutamine synthetase activities, and suggested a co-regulation of these traits.

Recently, genome-wide association studies (GWAS) have become a benchmark approach for fine-mapping QTL and postulating candidate genes. GWAS models are powerful tools for detecting QTLs by taking advantage of historical recombination events accumulated in diverse germplasm collections [26]. For NUE-related traits, GWAS have been conducted in wheat (*Triticum aestivum*) [27,28], winter rapeseed (*Brassica napus*) [7], maize [29] and Indian mustard [30]. In rapeseed seedlings, 14 QTL clusters were associated with 13 root- and biomass-related traits and NUE [31].

Whereas GWAS can identify putative genes associated with its detected QTLs, the gene expression patterns require further validation through gene expression studies, and

RNA sequencing (RNAseq) is a prime approach for such a validation. By combining GWAS and RNA-seq data, gene expression patterns for putative functional genes located within GWAS-identified QTL intervals have been reported and the involved biological processes more strongly validated than either strategy taken alone [32–34]. By cross-referencing the DEGs and GWAS-derived QTL-associated candidate genes, functional genes associated with harvest index-related traits in *Brassica napus* (rapeseed) [34], genes that co-modulate root traits and yield under drought in flax (*Linum usitatissimum*) [35], and genes that regulate root growth and NUE under depleted N conditions in rapeseed [31] have been reported.

Genomic selection (GS) is a strategy that is well suited to improve quantitative traits, particularly those with low heritability, as it makes use of all marker effects across the genome to calculate genomic estimated breeding values (GEBVs) for individuals' selection [36]. In traditional GS, prediction models of phenotypic traits using genome-wide markers are constructed based on a training population and then applied to test populations [37]. Using these models, the genetic effect values of unobserved individuals are predicted, allowing the use of some small-effect markers that would otherwise remain undetected in GWAS. An alternative strategy to genome-wide markers to predict GEBVs is to make use of markers obtained from GWAS, a variation of GS known as GWAS-assisted GS. GWAS removes a large proportion of unrelated markers, resulting in a limited number of favorable genetic loci linked to the trait of interest [38]. The predictive ability of GWAS-derived markers has been reported to be similar or superior to that attained using genome-wide markers in rice, citrus and flax [39–42].

Flax (*Linum usitatissimum* L.) is an important cash crop traditionally used as a natural fiber or oilseed crop with many health promoting attributes [43]. Its seed contains 40–45% oil, 20–25% protein, 20% insoluble fiber, 10% soluble fiber (mucilage) and 1% lignan secoisolariciresinol diglucosides (SDGs) [44]. Aside from being a rich source of functional ingredients, flax is a profitable option for many crop rotation scenarios. High-yielding flax production is achieved with 100–150 kg ha<sup>-1</sup> of N, accounting for 35–50% of its total production costs [45]. Therefore, an increased flax NUE will likely enhance its competitiveness with other crops, while minimizing its environmental footprint. Genetic variation in N accumulation, translocation and NUE has been reported in flax, and a moderate N supply (50–90 kg ha<sup>-1</sup>) was found to be adequate for promoting a maximum N translocation, NUE and oil production [46,47]. Whereas the detection of NUE variation in flax is promising, studies using genomic approaches including GWAS, RNA-seq and GS to decipher the genetic architecture of NUE have so far not been reported.

The objectives of the current study were to: (i) identify genetic loci associated with 21 NUE-related traits under optimal and deficient N conditions during the seedling stage of a flax association panel; (ii) generate and combine GWAS and RNA-seq data to identify candidate genes associated with root response under starved N conditions; and (iii) compare QTL markers and genome-wide SNPs for their GS prediction accuracies for NUE\_STI during the seedling stage in flax.

## 2. Results

### 2.1. Variations in Root and Biomass Phenotypic Traits

The REML analysis showed that N treatment and genotype were significant ( $p < 0.001$ ) for all traits except for the root dry weight (Table S2). The interaction between treatment and genotype was only found to be significant for shoot dry weight. Plants grown under N+ condition had statistically higher mean values for all traits, except for root/shoot ratio (R/S) and NUE, which showed higher mean values under N– conditions (Table 1). The R/S was 0.490 under N– treatment whereas plants grown under N+ had 0.407 as an R/S. The trait stability indices ranged from 76.1% (SDW\_Index) to 87.3% (TRL\_Index). The coefficients of variation for all traits were higher in the N– than under N+ treatment and ranged from 27.8 to 64.0% (Table 1). In general, the 21 NUE-related traits were normally distributed or close to normality (Figure 1).

**Table 1.** Phenotypic variation in 21 NUE-related traits under optimum and depleted N conditions in flax.

| Trait                             | Mean  | Standard Deviation | Range        | C.V. (%) |
|-----------------------------------|-------|--------------------|--------------|----------|
| Total root length N+ (cm)         | 469.2 | 137.7              | 168.6–882.0  | 29.2     |
| Total root length N– (cm)         | 407.2 | 156.8              | 171.0–870.9  | 38.3     |
| Root volume N+ (cm <sup>3</sup> ) | 0.464 | 0.181              | 0.161–1.056  | 38.7     |
| Root volume N– (cm <sup>3</sup> ) | 0.389 | 0.188              | 0.143–1.069  | 48.1     |
| Number of root tips N+            | 533.7 | 120.7              | 292.4–1060.4 | 22.5     |
| Number of root tips N–            | 447.8 | 125.1              | 236.6–864.5  | 27.8     |
| Plant dry weight N+ (mg)          | 105.7 | 52.9               | 11.8–390.9   | 49.8     |
| Plant dry weight N– (mg)          | 86.4  | 53.3               | 6.8–405.8    | 61.5     |
| Shoot dry weight N+ (mg)          | 77.1  | 41.3               | 9.1–290.6    | 53.3     |
| Shoot dry weight N– (mg)          | 59.9  | 38.5               | 4.6–280.0    | 64.0     |
| Root/shoot N+                     | 0.407 | 0.116              | 0.215–0.784  | 28.3     |
| Root/shoot N–                     | 0.490 | 0.158              | 0.188–0.862  | 32.0     |
| TRL_Index (%)                     | 87.3  | 21.6               | 53.1–172.4   | 24.7     |
| RV_Index (%)                      | 85.1  | 23.7               | 42.4–158.4   | 27.7     |
| RT_Index (%)                      | 84.6  | 16.9               | 53.9–131.8   | 19.9     |
| PDW_Index (%)                     | 80.1  | 21.1               | 28.7–156.9   | 26.2     |
| SDW_Index (%)                     | 76.1  | 22.9               | 22.9–166.7   | 30.0     |
| NUE N+                            | 25.6  | 7.2                | 10.4–37.2    | 28.0     |
| NUE N–                            | 28.3  | 7.8                | 13.7–46.5    | 27.5     |
| NUE_Index (%)                     | 114.6 | 25.0               | 59.7–204.7   | 21.7     |
| NUE_STI                           | 1.17  | 0.571              | 0.23–2.55    | 48.5     |

TRL: total root length; RV: root volume; RT: number of root tips; PDW: plant dry weight; SDW: shoot dry weight; NUE: nitrogen use efficiency; STI: stress tolerance index; C.V.: coefficient of variation.

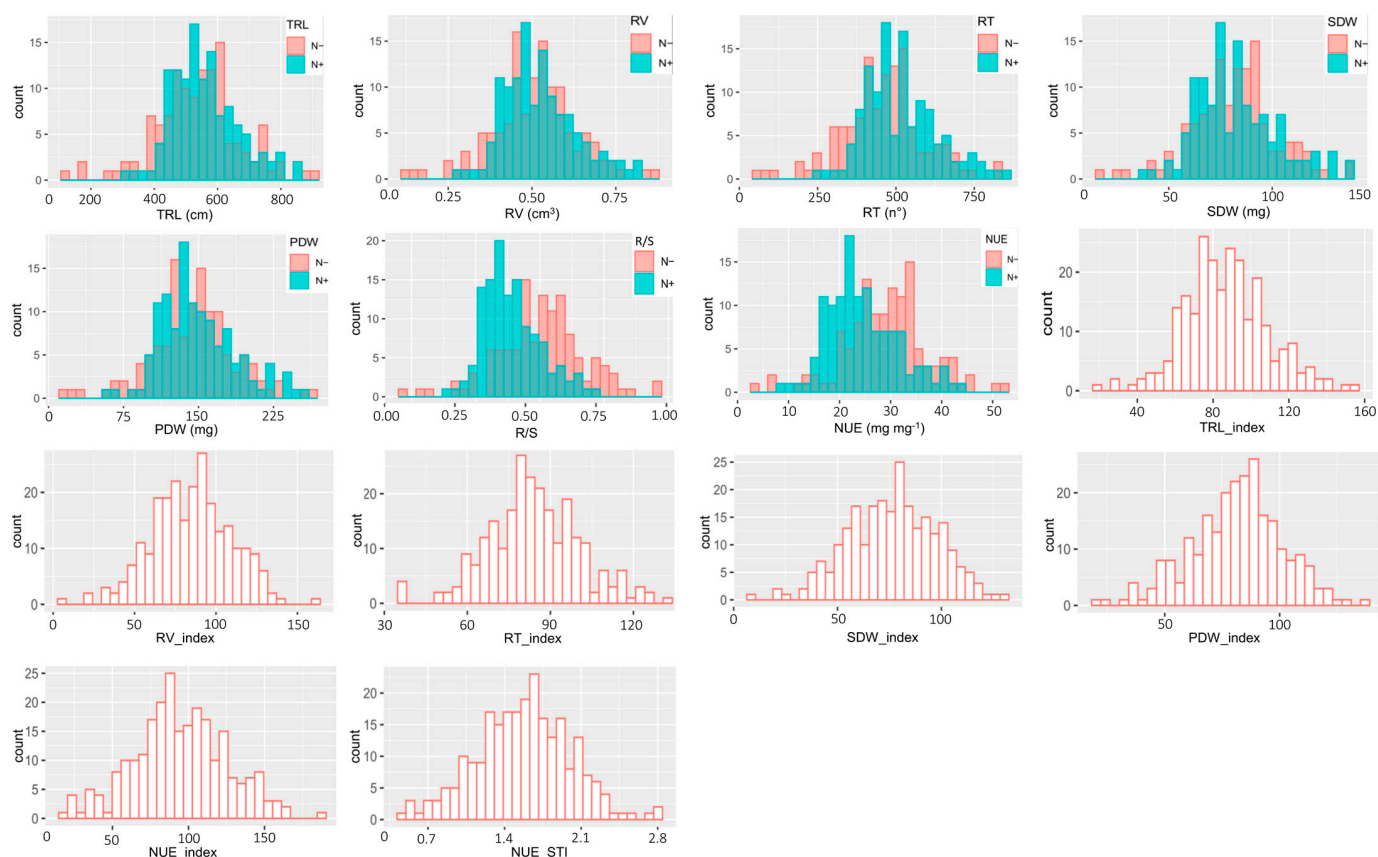


**Figure 1.** Phenotypic distribution of 21 NUE-related traits in flax including root and biomass traits, and trait indices under depleted N (N–) and optimum N (N+) conditions.



Moderate to high ( $p < 0.05$ ) correlation coefficients ( $r$ ) were observed between the root and biomass traits, and the stability indices under both N treatments ranged from 0.18 to 0.99 (Figure S1). Some stability indices were significantly ( $p < 0.05$ ) and negatively correlated with R/S\_N+, R/S\_N- and NUE\_N+. Root traits showed significant and positive correlations with NUE and NUE\_STI under both N conditions ( $r = 0.18$  to  $0.52$ ,  $p < 0.05$ ). Root volume (RV\_N-) and R/S\_N- were the most contributing traits to higher NUE under N stress, while R/S\_N- and RV\_N+ accounted for the most variation observed for NUE\_N+ (Figure S1). In contrast, biomass traits (SDW and PDW) did not show any significant correlation with NUE\_N-, NUE\_N+ and NUE\_STI.

## 2.2. Genetic Structure and Linkage Disequilibrium

The genetic structure analysis grouped the 123 flax accessions into two clusters (C1 and C2) as revealed by STRUCTURE (Figure 2a). The neighbor-joining (NJ) clustering and STRUCTURE produced similar outcomes, with the C2 accessions being the largest cluster (Figure 2b).

The kinship heatmap based on the identity by state (IBS) values showed the presence of three major clusters (Figure 2c). In general, intra group kinship was stronger than inter group kinship relationships among the 123 accessions, and the inter group kinship values were weaker than the intra group relationships.

The genome-wide LD decay was estimated to be 100 kb ( $r^2 = 0.1$ ) (Figure 2d). The chromosome-specific LD decays ( $r^2 = 0.1$ ) varied from 50 kb on chromosomes 4, 7 and 8 to 200 kb on chromosome 13 (Figure S2). The LD decay used for grouping QTNs into QTL ( $r^2 > 0.3$ ) for chromosomes harboring QTNs ranged from 10 kb on chromosome 4 to 40 kb on chromosome 13 with a mean of 14.3 kb (Figure S2).

## 2.3. ML-GWAS of 21 NUE-Related Traits in Flax

The multi-locus methods identified 552 unique QTNs associated with at least one of the 21 traits (Figures 3 and S3). The mrMLM, FASTmrMLM, ISIS EM-BLASSO, FASTmrEMMA and pLARmEB methods detected 64, 231, 91, 32 and 134 of the 552 QTNs, respectively, but some were identified by more than one model. Mann-Whitney non-parametric U tests were conducted on the 552 unique QTNs and the 76 non-significant ones were removed, resulting in a subset of 476 QTNs ( $p < 0.05$ ), which was subsequently merged into 359 QTL based on the LD criteria ( $r^2 > 0.3$ ) as defined previously. The 359 QTL individually explained 0.11% to 23.07% of the phenotypic variation for the 21 NUE-related traits (Table S3). Of these, 124 were detected by at least two models, and 40 were considered major QTLs as they explained more than 10% of the phenotypic variation ( $R^2$ ). One hundred ten QTLs were pleiotropic with at least two traits, which were generally highly correlated. For example, QTL Lu13\_19514686 was associated with eight traits, including NUE\_N-, RV\_N-, PDW\_N-, SDW\_N-, TRL\_N+, RV\_N+, RT\_N+ and PDW\_N+, with correlation coefficients ranging from 0.40 to 0.99 and an  $R^2$  ranging from 2.41 to 12.85% (Table S3, Figure S1).

Simple regression analyses of QTLs for traits revealed moderate to high mean percentage of phenotypic variation explained ( $\text{adj}R^2$ ), with 0.61, 0.69 and 0.70 for traits under N-, N+ and stability indices, respectively (Figures 4 and S4). QTLs identified under N- explained 42% (SDW\_N-) to 75% (RT\_N-) of the phenotypic variation, while QTLs detected under N+ condition accounted for 56% (PDW\_N+) to 78% (TRL\_N+ and R/S\_N+). QTLs associated with stability indices explained 58% (PDW\_Index) to 77% (TRL\_Index) of the traits' variation (Figures 4 and S4).

The top 10% of accessions (12/123), corresponding to the group of accessions with the highest NUE\_N-, and the bottom 10%, corresponding to the group of accessions with the lowest NUE\_N-, showed an average NUE\_N- of 38.2 (range 26.9 to 46.1) and 19.5 (range 13.7 to 24.7), respectively. Accessions with the highest NUE\_N- had, on average, 11 PQTLs (range 10 to 11) associated with this trait, while the genotypes with the lowest NUE\_N- had on average four PQTLs (ranging from two to five). The oilseed-

type accession O\_IRL\_C\_CN98192 from Ireland had the highest NUE<sub>N</sub> value of 46.1 and contained 331 PQTLs, whereas the Indian accession O\_IND\_C\_CN98982 registered a NUE<sub>N</sub> of 18.1 and had 261 PQTLs out of the 359 identified for the 21 NUE-related traits. O\_IRL\_C\_CN98192 and O\_IND\_C\_CN98982 registered NUE<sub>STI</sub> values of 2.55 and 0.33, respectively, suggesting that O\_IRL\_C\_CN98192 has a high NUE and high nitrogen responsive cultivar while O\_IND\_C\_CN98982 has a low NUE and a low nitrogen responsive genotype. These two accessions were selected for root transcriptome analysis.

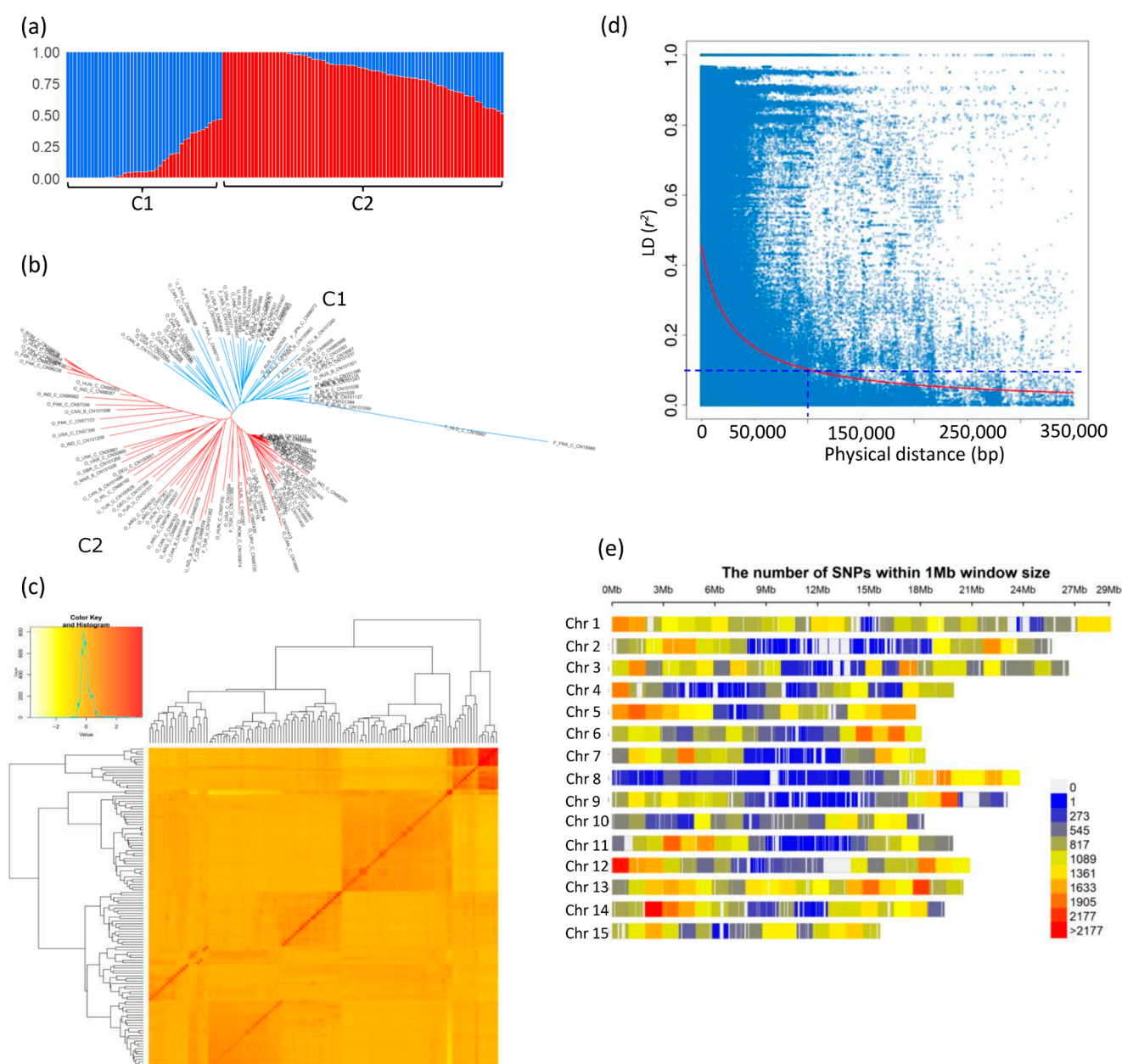


**Figure 2.** (a) Model-based population structure of 123 flax accessions belonging to two clusters predefined by the STRUCTURE software. (b) Neighbor-joining (NJ) tree of 123 flax accessions based on the 272,944 SNPs. (c) Kinship relationships among the 123 flax accessions of the collection. (d) Genome-wide linkage disequilibrium (LD) decay of  $r^2$  values (red line), against physical distance (bp) in flax. The dashed blue line indicates the cutoff value ( $r^2 = 0.1$ ) used to determine the genome-wide LD block size. (e) Distribution of 272,944 SNPs used for GWAS analysis across the 15 *Linum usitatissimum* chromosomes. C1: cluster 1; C2: cluster 2.

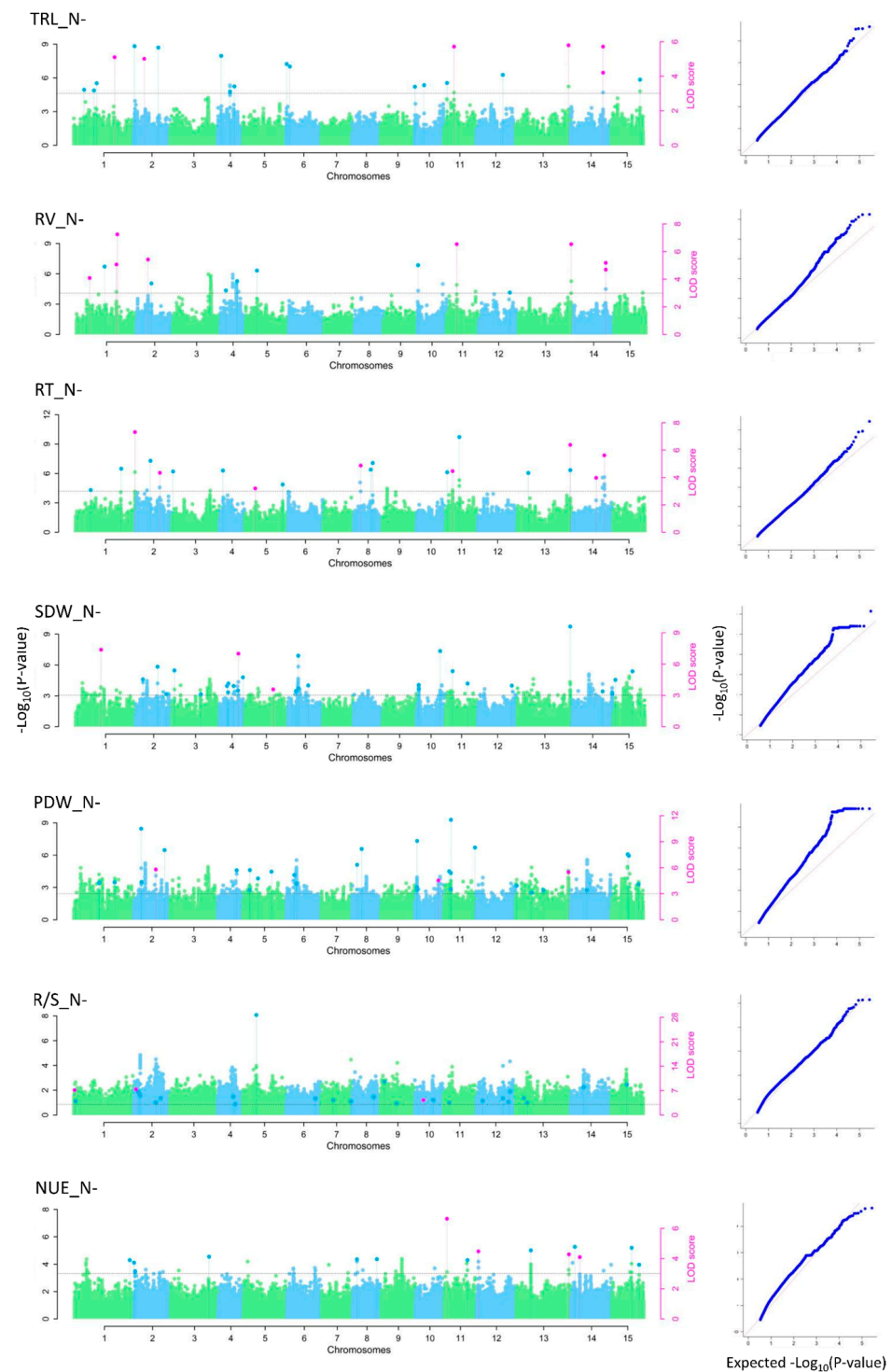


**Figure 3.** Manhattan (left panels) and quantile–quantile (Q-Q) plots (right panels) of multi-locus GWAS models of NUE-related traits. QTNs commonly identified by multiple approaches are indicated by the pink dots shown above dotted vertical lines; QTNs identified by a single model are represented by blue dots above vertical lines. The grey horizontal dotted line indicates the genome-wide significance threshold  $-\log_{10}(p)$  equivalent to the  $\text{LOD} > 3.0$  for ML-GWAS models. TRL\_N–: total root length under N–; RV\_N–: root volume under N–; RT\_N–: number of root tips under N–; SDW\_N–: shoot dry weight under N–; PDW\_N–: plant dry weight under N–; R/S\_N–: root-to-shoot ratio under N–.

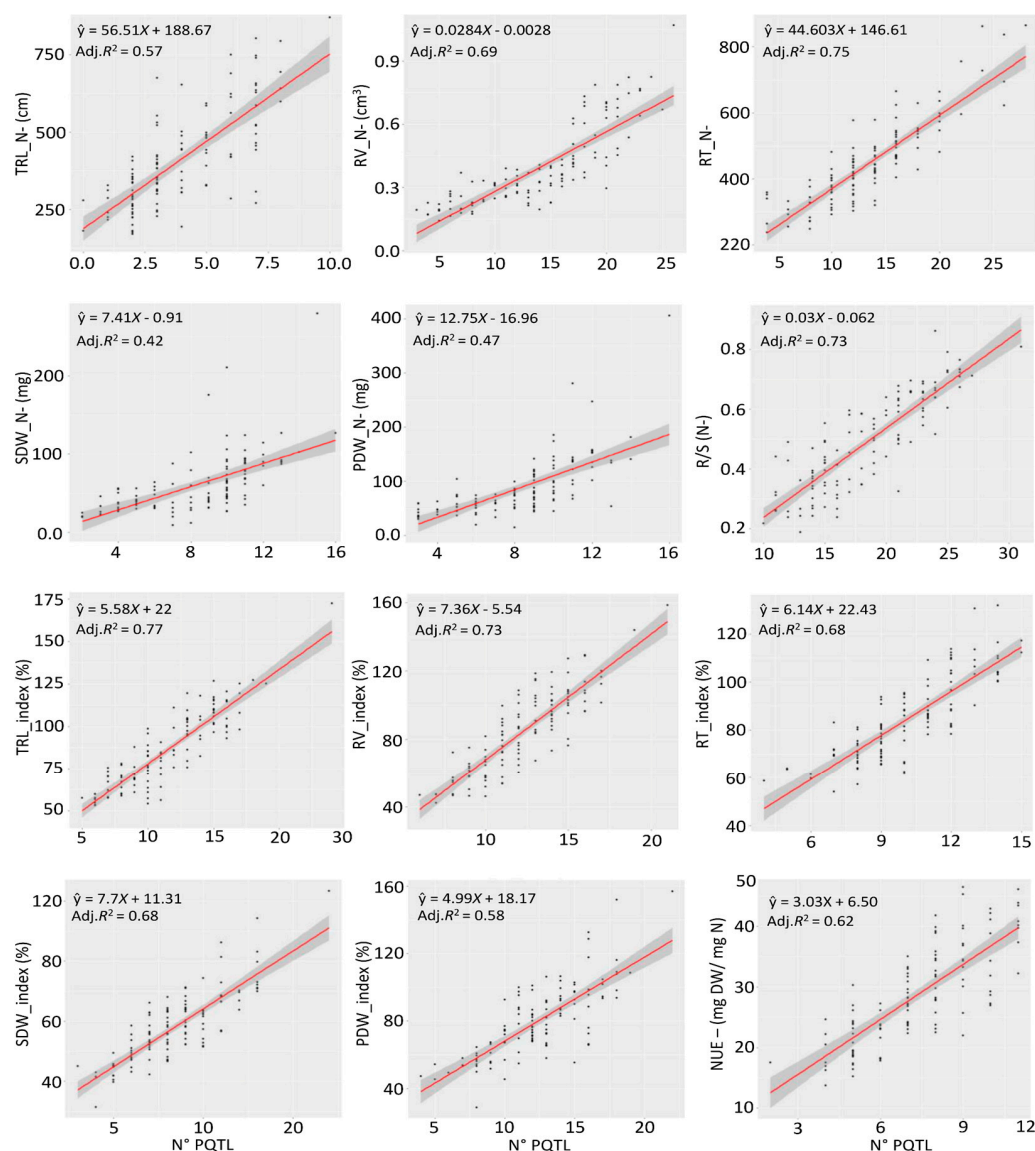


**Figure 4.** Simple regression analyses of QTL on trait for NUE-related traits and the phenotypic variation explained ( $\text{adj}R^2$ ) for all detected QTL for each individual trait. TRL\_N-: Total root length under N-, RV\_N-: Root volume under N-, RT\_N-: Number of root tips under N-, SDW\_N-: Shoot dry weight under N-, PDW\_N-: Plant dry weight under N-, R/S\_N-: Root to shoot ratio under N-, TRL\_Index: Total root length index, RV\_Index: Root volume index, RT\_Index: Number of root tips index, SDW\_Index: Shoot dry weight index, PDW\_Index: Plant dry weight index, NUE\_N-: Nitrogen use efficiency under N-.

#### 2.4. Differentially Expressed Genes between High and Low NUE Genotypes

A total of 16 libraries, representing two genotypes, two treatments and four biological replicates, were sequenced on an Illumina NovaSeq 6000 platform (San Diego, CA, USA) using the 150 bp paired end read mode, resulting in a total of 411,296,419 million raw reads. After removal of low-quality reads with Trimmomatic v.1.0 402,733,447 high quality reads were found, of which 376,423,963 (92.11%) were mapped to the flax (*L. usitatissimum*) reference genome [48] (Table S4).

Using a principal component analysis (PCA) of gene expression levels, the correlation between biological replicates within the same genotype was greater than the correlation between biological replicates between HN and LN genotypes (Figure S5), which was in agreement with the contrasting N response between genotypes and highlights the accuracy of the four biological replicates.



Root transcriptome differences between HN and LN genotypes after 15 days of N deficiency were determined by performing comparisons between the aligned reads of N– and N+ treatments. A total of 1034 DEGs were identified, of which 108 and 926 were detected in HN and LN genotypes, respectively (Table S5, Figure S6). Among the 108 DEGs observed in HN, 66 and 42 were up and down regulated, respectively. The LN genotype registered 988 DEGs, of which 286 and 702 were up and down regulated, respectively (Table S5, Figure S6).

KEGG enrichment analysis revealed 104 and 223 significantly enriched pathways associated with the up- and down regulated genes, respectively. Among the most enriched pathways, metabolic pathways (map01100), biosynthesis of secondary metabolites (map01110), plant–pathogen interaction (map04626), MAPK signaling plant pathway (map04016), plant hormone signal transduction (map04075), diterpenoid biosynthesis including gibberellin biosynthesis (map00904) and nitrogen metabolism (map00910) were represented more among the up-regulated DEGs (Figure S7a). The KEGG metabolic pathways (map01100), biosynthesis of secondary metabolites (map01110), MAPK signaling plant pathway (map04016), plant–pathogen interaction (map04626), plant hormone signal transduction (map04075), microbial metabolism in diverse environments (map01120) and starch and sucrose metabolism (map00500) were represented more among the down-regulated DEGs (Figure S7b).

Among the DEGs identified, *cytokinin response factor 4* (CRF4, *Lus10039324*) and *nitrate regulatory gene2* (NRG2, *Lus10029683*) were involved in N signaling (Tables 2 and S6). DEGs participating in nitrate assimilation, such as *NITRATE TRANSPORTER1/PEPTIDE TRANSPORTER3.1* (NPF3.1, *Lus10041466*), *nitrate reductase* (NIA, *Lus10035402*) and *SNF1-related protein kinase regulatory subunit beta-2* (KINB2, *Lus10038783*), registered altered gene expression patterns in roots in the LN genotype. Genes encoding nitrate transporters like *NITRATE TRANSPORTER1/PEPTIDE TRANSPORTER1.1* (NPF1.1/NRT1.12, *Lus10014537*), *NITRATE TRANSPORTER1/PEPTIDE TRANSPORTER6.3* (NPF6.3/NRT1.1, *Lus10032252*) and the *high-affinity nitrate transporter NRT2.1* (NRT2.1, *Lus10016120*) were observed in LN roots. Several genes involved in root development, like *NAC021* (*Lus10024908*), *MYB77* (*Lus10010238*) and *WRKY75* (*Lus10011346*) transcription factors, *C-TERMINALLY ENCODED PEPTIDE RECEPTOR 2* (CEPR2, *Lus10012461*), *ARABIDOPSIS CRINKLY4* (ACR4, *Lus10025455*), *Super Numeric Nodules* (SUNN, *Lus10040592*) and *multidrug resistance protein 4* (MDR4, *Lus10010012*) were solely transcriptionally altered in the LN accession (Table 2). Various genes involved in amino acid transport also exhibited differential expression patterns, and include *gamma-glutamyl cyclotransferase 2.1* (GGCT2.1, *Lus10020181*), *amino acid transporter AAP3* (AAP3, *Lus10042740*) and *BASIC AMINO ACID CARRIER 2* (BAC2, *Lus10011451*) (Tables 2 and S6). Notably, 89.5% of the DEGs were down regulated in the root transcriptome of the LN genotype as compared to the HN accession, in agreement with its reduced NUE\_STI (Tables 2 and S6).

**Table 2.** Differentially expressed genes involved in NUE-related traits in flax functionally that have been validated in other plant studies.

| Flax DEG           | Gene Name     | Protein Name  | QTL           | Trait                   | Function   | Up/Down (Log <sub>2</sub> FC)       | Reference |
|--------------------|---------------|---|---------------|-------------------------|--|-------------------------------------|-----------|
| <i>Lus10027573</i> | <i>CRF4</i>   | Ethylene-responsive transcription factor CRF4         | Not in QTL    | Unknown                 | N signaling  | Up LN (1.20)                        | [49]      |
| <i>Lus10029683</i> | <i>NRG2</i>   | Nitrate regulatory gene2 protein                      | Lu9_18443162  | RV_Index                | N signaling  | Down LN (−1.33)                     | [50]      |
| <i>Lus10019292</i> | <i>LBD38</i>  | LOB domain-containing protein 38                      | Not in QTL    | Unknown                 | NO <sub>3</sub> <sup>−</sup> response regulation               | Up LN (1.27)                        | [51]      |
| <i>Lus10038783</i> | <i>KINB2</i>  | SNF1-related protein kinase regulatory subunit beta-2 | Lu11_1841121  | NUE_N−, NUE_N+, NUE_STI | NO <sub>3</sub> <sup>−</sup> assimilation                      | Down LN (−1.32)                     | [52]      |
| <i>Lus10041466</i> | <i>NPF3.1</i> | Protein NRT1/PTR FAMILY 3.1                           | Lu4_14298191  | R/S_N−                  | NO <sub>3</sub> <sup>−</sup> assimilation                      | Up LN (1.49)                        | [53]      |
| <i>Lus10035402</i> | <i>NIA</i>    | Nitrate reductase [NADH]                              | Not in QTL    | Unknown                 | NO <sub>3</sub> <sup>−</sup> assimilation                      | Down LN (−1.26)                     | [54]      |
| <i>Lus10027270</i> | <i>NR</i>     | Nitrate reductase [NADH]                              | Not in QTL    | Unknown                 | NO <sub>3</sub> <sup>−</sup> assimilation                      | Down LN (−1.46)                     | [55]      |
| <i>Lus10004037</i> | <i>GS1-2</i>  | Glutamine synthetase cytosolic isozyme 2              | Not in QTL    | Unknown                 | NH <sub>4</sub> <sup>+</sup> assimilation                      | Down LN (−1.37),<br>Down HN (−1.03) | [56]      |
| <i>Lus10029256</i> | <i>CEP14</i>  | Precursor of CEP14                                    | Not in QTL    | Unknown                 | NH <sub>4</sub> <sup>+</sup> assimilation,<br>root development | Down LN (−1.16)                     | [57]      |
| <i>Lus10016120</i> | <i>NRT2.1</i> | High-affinity nitrate transporter 2.1                 | Not in QTL    | Unknown                 | NO <sub>3</sub> <sup>−</sup> transporter                       | Down LN (−1.17)                     | [58]      |
| <i>Lus10030902</i> | <i>NRT2.5</i> | High affinity nitrate transporter 2.5                 | Lu13_18363934 | RT_Index, R/S_N+        | NO <sub>3</sub> <sup>−</sup> transporter                       | Down LN (−2.38),<br>Down HN (−1.83) | [59]      |
| <i>Lus10014537</i> | <i>NPF1.1</i> | Protein NRT1/PTR FAMILY 1.1                           | Not in QTL    | Unknown                 | NO <sub>3</sub> <sup>−</sup> transporter                       | Up LN (1.12)                        | [18]      |
| <i>Lus10032876</i> | <i>NPF4.6</i> | Protein NRT1/PTR FAMILY 4.6                           | Not in QTL    | Unknown                 | NO <sub>3</sub> <sup>−</sup> transporter                       | Down LN (−1.06)                     | [60]      |
| <i>Lus10032252</i> | <i>NPF6.3</i> | Protein NRT1/PTR FAMILY 6.3                           | Not in QTL    | Unknown                 | NO <sub>3</sub> <sup>−</sup> transporter                       | Down LN (−1.21)                     | [58]      |
| <i>Lus10004760</i> | <i>AMT1-2</i> | Ammonium transporter 1 member 2                       | Lu14_9866805  | RV_N−                   | NH <sub>4</sub> <sup>+</sup> transporter                       | Down LN (−3.14),<br>Down HN (−2.20) | [61]      |

Table 2. Cont.

| Flax DEG           | Gene Name     | Protein Name   | QTL           | Trait            | Function         | Up/Down (Log <sub>2</sub> FC)       | Reference |
|--------------------|---------------|--|---------------|------------------|------------------|-------------------------------------|-----------|
| <i>Lus10008564</i> | <i>ACO1</i>   | 1-aminocyclopropane-1-carboxylate oxidase 1            | Lu11_14898826 | NUE_N–           | Root development | Up LN (1.04)                        | [62]      |
| <i>Lus10036251</i> | <i>GSO1</i>   | LRR receptor-like serine/threonine-protein kinase GSO1 | Lu12_1386203  | RT_N+, R/S_N–    | Root development | Up LN (1.91)                        | [63]      |
| <i>Lus10016554</i> | <i>FLA4</i>   | Fasciclin-like arabinogalactan protein 4               | Lu12_4334157  | PDW_N+           | Root development | Down LN (–1.02)                     | [64]      |
| <i>Lus10011346</i> | <i>WRKY75</i> | Probable WRKY transcription factor 75                  | Lu13_19862281 | TRL_Index        | Root development | Up LN (1.46)                        | [65]      |
| <i>Lus10042154</i> | <i>FH8</i>    | Formin-like protein 8                                  | Lu14_15927781 | RV_N+            | Root development | Up LN (1.53)                        | [66]      |
| <i>Lus10021428</i> | <i>MYB36</i>  | Transcription factor MYB36                             | Lu14_3980668  | R/S_N–           | Root development | Down LN (–1.02)                     | [67]      |
| <i>Lus10035126</i> | <i>RPK2</i>   | LRR receptor-like serine/threonine-protein kinase RPK2 | Lu2_21668160  | PDW_N+           | Root development | Down LN (–1.28)                     | [63]      |
| <i>Lus10024314</i> | <i>BZIP29</i> | bZIP transcription factor 29                           | Lu6_17695007  | NUE_N+, R/S_N+   | Root development | Down LN (–1.06)                     | [68]      |
| <i>Lus10024908</i> | <i>NAC021</i> | NAC domain-containing protein 21/22                    | Lu9_19469655  | R/S_N–, RV_Index | Root development | Up LN (1.20)                        | [69]      |
| <i>Lus10031059</i> | <i>MIZ1</i>   | Protein MIZU-KUSSEI 1                                  | Lu9_6368499   | NUE_N+           | Root development | Down LN (–1.54),<br>Down HN (–1.40) | [70]      |
| <i>Lus10012461</i> | <i>CEPR2</i>  | Receptor protein-tyrosine kinase CEPR2                 | Not in QTL    | Unknown          | Root development | Up LN (1.08)                        | [71]      |
| <i>Lus10010238</i> | <i>MYB77</i>  | Transcription factor MYB77                             | Not in QTL    | Unknown          | Root development | Down LN (–1.22)                     | [72]      |
| <i>Lus10040274</i> | <i>LBD29</i>  | LOB domain-containing protein 29                       | Not in QTL    | Unknown          | Root development | Up LN (1.80)                        | [73]      |
| <i>Lus10025455</i> | <i>ACR4</i>   | Serine/threonine-protein kinase-like protein ACR4      | Not in QTL    | Unknown          | Root development | Up LN (1.63)                        | [74]      |
| <i>Lus10040592</i> | <i>SUNN</i>   | Leucine-rich repeat receptor-like kinase protein SUNN  | Not in QTL    | Unknown          | Root development | Down LN (–1.32)                     | [75]      |

Table 2. Cont.

| Flax DEG           | Gene Name      | Protein Name                            | QTL           | Trait               | Function             | Up/Down (Log <sub>2</sub> FC)       | Reference |
|--------------------|----------------|---|---------------|---------------------|----------------------|-------------------------------------|-----------|
| <i>Lus10017271</i> | <i>ABCB19</i>  | ABC transporter B family member 19      | Not in QTL    | Unknown             | Root development     | Up LN (1.52)                        | [76]      |
| <i>Lus10010012</i> | <i>ABCB4</i>   | ABC transporter B family member 4       | Not in QTL    | Unknown             | Root development     | Down LN (−1.06)                     | [77]      |
| <i>Lus10005574</i> | <i>CAT8</i>    | Cationic amino acid transporter 8       | Lu14_17132252 | R/S_N+              | Amino acid transport | Up LN (1.15)                        | [78]      |
| <i>Lus10020181</i> | <i>GGCT2.1</i> | Gamma-glutamyl cyclotransferase 2.1     | Lu2_4220131   | TRL_Index, RT_Index | Amino acid transport | Up LN (1.38)                        | [79]      |
| <i>Lus10029533</i> | <i>BAT1</i>    | Amino-acid permease BAT1 homolog        | Not in QTL    | Unknown             | Amino acid transport | Up LN (1.12)                        | [80]      |
| <i>Lus10012824</i> | <i>AVT1J</i>   | Amino acid transporter AVT1J            | Not in QTL    | Unknown             | Amino acid transport | Up LN (1.72)                        | [81]      |
| <i>Lus10008910</i> | <i>GDU5</i>    | Protein GLUTAMINE DUMPER 5              | Not in QTL    | Unknown             | Amino acid transport | Down LN (−1.20),<br>Down HN (−1.99) | [82]      |
| <i>Lus10042740</i> | <i>AAP3</i>    | Amino acid permease 3                   | Not in QTL    | Unknown             | Amino acid transport | Down LN (−1.49)                     | [83]      |
| <i>Lus10011451</i> | <i>BAC2</i>    | Mitochondrial arginine transporter BAC2 | Not in QTL    | Unknown             | Amino acid transport | Down LN (−1.23)                     | [84]      |
| <i>Lus10015513</i> | <i>GDU3</i>    | Protein GLUTAMINE DUMPER 3              | Not in QTL    | Unknown             | Amino acid transport | Down LN (−1.19)                     | [85]      |

LN: low NUE genotype; HN: high NUE genotype.



### 2.5. Differentially Expressed Candidate Genes at QTLs

The 359 unique QTLs were mined for the identification of differentially expressed candidate genes involved in nitrogen stress responses. The linkage disequilibrium blocks ( $\pm 100$  kb) in the detected QTLs harbored 13,683 genes. Using RNA-seq data from the two NUE contrasting flax accessions, a total of 337 DEGs (32.6%) were found within 169 of these QTL windows (Table S6). The number of DEGs per QTL windows ranged from one to six, with an average of  $2 \pm 1.04$  per QTL. For example, Lu1\_9831112 QTL associated with TRL\_Index explained 8.7% of the phenotypic variation, and harbored *CBL-interacting serine/threonine-protein kinase 14* (*CIPK14*, *Lus10022748*), the expression of which was increased ~4-fold in LN and nearly doubled in HN under N+ condition compared to N-. (Table 2, Figure 5). Similar trends were observed for Lu2\_4220131, a QTL associated with RT\_Index that accounted for 11.1% of the phenotypic variation and which carried *gamma-glutamylcyclotransferase 2.1* (*GGCT2.1*, *Lus10020181*), whose expression was increased 2.5-fold in LN under N+ condition compared to N-, whereas in HN the expression patterns were not statistically altered (Figure 5).

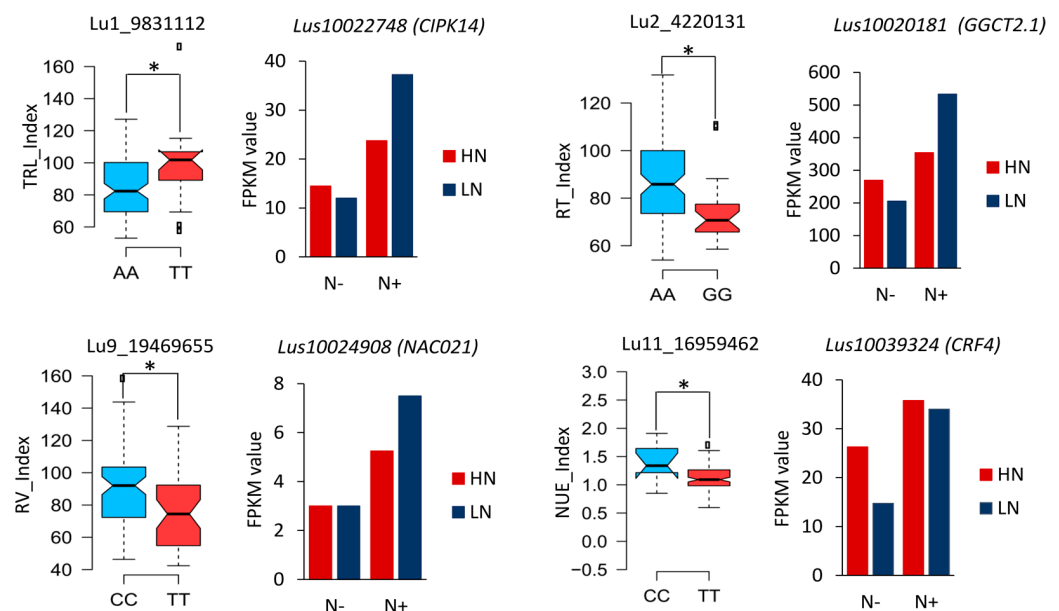


**Figure 5.** Effects of quantitative trait locus of some NUE-related QTL harboring differential expressed genes (DEGs) identified under contrasting N conditions. Box plots (**left panels**) showing the allelic effect of QTLs associated with NUE-related traits harboring DEGs involved in NUE responses identified in other plant species. Graphics (**right panels**) showing DEGs in QTLs identified under contrasting N conditions in high NUE (HN) and low NUE (LN) flax accessions. FPKM: Fragments per kilobase million. \* statistically significant at  $p < 0.05$ .

The root-development associated DEG NAC021 was located in the pleiotropic QTL Lu9\_19469655 associated with R/S\_N- and the RV\_Index. The expression of NAC021 increased 2.5-fold in LN and nearly doubled in HN under N+ condition compared to N-. Another example of QTL harboring DEGs involved in N stress responses was Lu11\_16959462, associated with the NUE\_Index, which harbored the N signaling gene CRF4, whose expression patterns were not significantly altered in HN, but increased ~twofold in LN under N+ conditions compared to N-. (Figure 5, Table S6). In addition, QTL Lu4\_14298191 linked to R/S\_N- harbored the nitrate transporter NPF3.1. The DEG high affinity nitrate transporter 2.5 (NRT2.5) was located in the pleiotropic QTL Lu13\_18363934 which is associated with the RT\_Index and R/S\_N+ (Tables S3 and S6). In general, most of the DEGs in QTLs exhibited altered expression patterns in the LN genotype, but stable expression under N- and N+ conditions in the HN accession.

## 2.6. GWAS-Assisted Genomic Selection

To identify the marker sets that produce the best prediction accuracy for NUE\_STI, the predictive ability of five marker sets (M1 = 16,383 genome-wide markers; M2 = markers associated with all traits under N– condition; M3 = markers associated with NUE\_STI; M4 = markers associated with all traits positively correlated with NUE\_STI; and M5 = markers associated with all traits positively correlated with NUE\_STI that harbored DEGs) were compared using the GS GBLUP model. Analysis of variance in prediction accuracy for the five marker sets showed significant differences ( $p < 0.001$ ). Tukey's multiple pairwise comparisons showed the highest predictive ability for M3 ( $r = 0.79$ ), followed by M4 ( $r = 0.76$ ) (Figure 6). The predictive ability obtained from the other marker sets was significantly lower, with the lowest observed using M1 ( $r = 0.11$ ) (Figure 6).

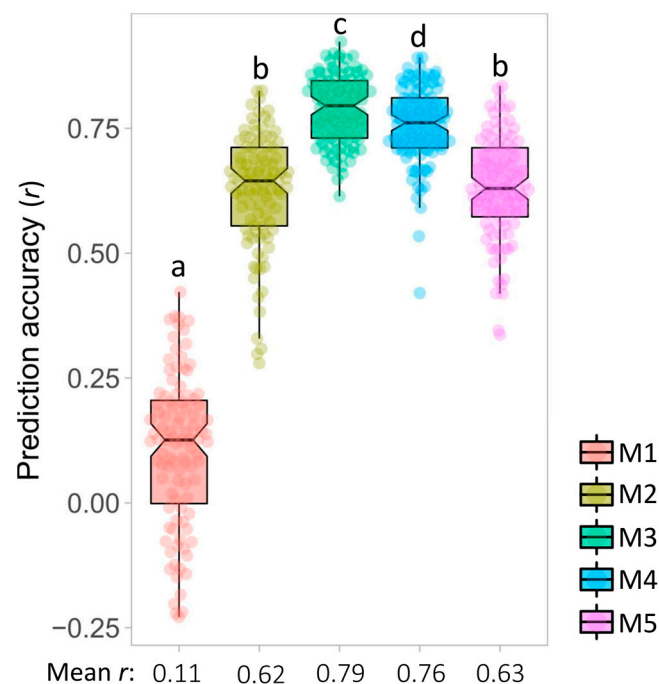


**Figure 6.** Comparison of genomic prediction accuracy ( $r$ ) models produced by five different marker sets using the GBLUP statistical model for NUE\_STI in flax. M1: marker set 1 using 16,383 genome-wide markers, M2: marker set 2 considering markers associated with all traits under N– condition, M3: marker set 3 including markers associated with NUE\_STI, M4: marker set 4 considering markers associated with traits positively correlated with NUE\_STI, M5: marker set 5 including markers associated with traits positively correlated with NUE\_STI that harbor DEGs. Box plots with the same lowercase letter are not statistically significant at  $p < 0.05$ .

## 3. Discussion

Nitrogen plays an important role in root and shoot development and is a critical macronutrient for maximizing yield. Lowering N input and breeding plants with higher NUE are main goals of plant nutrition and sustainable agriculture [9]. Here, we assessed 21 NUE-related traits under N– and N+ conditions for 123 diverse flax accessions during the seedling stage using a multi-omics approach combining GWAS, RNA-seq and GS to understand the flax nitrogen's response to depleted N conditions and to apply future genomic-assisted breeding strategies.

### 3.1. Phenotypic Variation of Root and Biomass Traits

The concepts of high and low NUE genotypes are widely used in N use efficiency studies. Nonetheless, one must bear in mind that high or low NUE ranking is a relative measurement in comparison to other genotypes within the same experiment. Hence, a high NUE genotype in one study could be a low NUE accession in another depending on the

genetic diversity of the panel [42]. In flax, NUE traits and optimum N dosages for efficient flax production have been investigated using, at most, a dozen cultivars [46,47], limiting their broad deployment in breeding programs. Here, an association panel of 123 flax accessions representing the genetic diversity from 28 countries was assembled from the Canadian flax core collection [86], including eighty-three cultivars, twenty-one breeding lines and five landraces that encompass both the oil and fiber morphotypes. The significant and broad variation in root and biomass traits among the genotypes of the association panel agrees with previous studies of similar traits using subsets of the Canadian flax core collection [35,45,87,88]. Thus, this set of flax accessions was considered suitable as a diverse genetic resource for identifying high NUE donor lines for breeding.

Plants grown under N− conditions showed, on average, reduced root and shoot trait values, but increased R/S\_N− and NUE\_N− than plants grown under N+ conditions, indicating that N-depleted plants can mobilize more carbon to promote root development and, consequently, mine the substrate to acquire N [10,31,42]. In most elite cultivars, increasing the root-to-shoot ratio increases the uptake of N from the deep soil because the longer roots provide optimum nutrient storage in shoots that can be used later at the seed filling stage [89]. The significant and positive correlations between NUE and root traits ( $r = 0.33$  to  $0.52$ ) require breeders to consider root traits as selection criteria to improve NUE in flax breeding programs, as observed in maize [10] and rapeseed [31]. Therefore, the selection of optimal root traits, and particularly R/S\_N−, at the seedling stage, holds promises to optimize flax NUE.

### 3.2. Genetic Structure and Linkage Disequilibrium

Understanding the genetic structure and extent of LD in germplasm resources is crucial for conducting reliable GWAS. Population structure and cryptic relatedness (kinship) are the main factors influencing the number of false marker–trait associations, while LD is the main factor influencing marker density requirement and mapping resolution in association studies [90]. Here, we observed weak kinship relationships among accessions and rapid LD decay for most of the chromosomes. The 123 flax accessions are expected to contain ample allelic diversity, as suggested by the generally small LD blocks for the 15 chromosomes, thereby minimizing the occurrence of false positives and facilitating the search of N stress candidate genes through efficiently narrowing the putative QTL regions.

### 3.3. ML-GWAS of 21 NUE-Related Traits in Flax

Each step contributing to NUE, such as uptake, translocation, assimilation and remobilization of N, is a complex process controlled by many molecular, physiological and metabolic root- and shoot-related traits that may exert independent or synergistic effects on NUE, complicating the comprehensive dissection of its genetic architecture. GWAS has become a widely used method for the genetic dissection of complex traits like NUE-related traits in *Triticum aestivum* (wheat) [28,91], *Zea mays* (maize) [29,92], *Brassica napus* (rapeseed) [7,31] and *Hordeum vulgare* (barley) [93]. In flax, GWAS have been conducted for agronomic, seed quality and disease resistance traits [94–97], as well as for drought-related traits and early root and shoot development [35,87,88,98].

Using six ML-GWAS models, 359 unique QTLs, distributed over all 15 chromosomes, were detected for 21 NUE-related traits. Multi-locus models consider multiple QTLs in the model and treat them as random effect, which assumes that multiple QTLs control the phenotype [99]. Because all the potential QTLs for the quantitative traits are fitted to a single linear model and their effects are estimated and tested simultaneously, the classical stringent Bonferroni correction is unwarranted because the detection of many small effect QTLs is key to detect the full breadth of the QTLs underlying complex traits [95]. To maximize the robustness and reliability of the significant marker-trait associations, the Mann–Whitney non-parametric U tests were carried out to remove false positive QTLs that did not produce a significant allelic effect on the traits. In flax, this approach has been applied for flowering time [100], root and shoot development [87,88,98], drought-related

traits [35,87] and disease resistance traits [95,101], totaling 1478 QTLs identified, allowing for their application in GWAS-assisted genomic selection strategies [41,95,101].

The high number of pleiotropic QTLs ( $n = 110$ ) indicates the close genetic relationships between most of the 21 traits assessed (Table 2). Importantly, NUE and root traits were co-located at fifteen pleiotropic QTLs, whereas NUE and shoot traits shared the same genomic regions at only three QTLs. The important genetic associations between root traits and NUE are not only seen in the seedling stage, but also at the reproductive stage, as previously reported in other crops [10,31,102]. Accordingly, the significant relationships found between root QTLs and yield under water stress in flax [35] and phosphorus deficiency in maize [103] further support the essential role of root traits on adaptation of crops to abiotic stresses.

### 3.4. Differentially Expressed Genes between High and Low NUE Genotypes

The RNA-seq approach has been applied in many crops for multiple traits to identify gene networks [104]. Here, we identified 1034 DEGs in the roots of two flax genotypes with contrasting NUE, where most genes showed altered patterns of expression in the low NUE (LN) genotype. KEGG pathway analysis showed that DEGs involved in metabolic pathways, the biosynthesis of secondary metabolites, plant–pathogen interaction and some genes involved in N metabolism and phenylpropanoid biosynthesis were significantly enriched. Key metabolic processes such as energy production, N assimilation and root development, among others, were repressed in LN, while they remained unaltered in HN, indicating its greater potential to cope with N depleted environments. Similar KEGG pathway results in roots submitted to N starved conditions have been reported in rice [105] and cotton [106].

Our study provides the first insight into N stress-responsive genes hypothesized to have important roles in N stress adaptation in flax. The distinct transcriptional response observed in both flax accessions in response to starved N condition may serve as a roadmap to understanding the genetic factors and their interactions in governing NUE in flax.

Through gene annotation and literature reports, at least fifteen identified DEGs are involved in N metabolism, of which ten were downregulated in LN. For instance, a mutation in *AtNRG2*, the *Arabidopsis* ortholog of flax *Lus10029683*, disrupted the induction of nitrate-responsive genes after nitrate treatment, where the nitrate content in roots was lower in the mutants than in the wild type [50]. The reduced nitrate content in roots may have resulted from a reduced expression of *NPF6.3/NRT1.1*, the *Arabidopsis* ortholog of flax *Lus10032252*. *NPF6.3/NRT1.1* is a bidirectional transporter involved in root-to-shoot nitrate translocation [58], which was also downregulated in LN. Root traits play a pivotal role in response to N stress and superior NUE in plants. Here, we identified seventeen DEGs that modulate root development, of which nine were involved in lateral root development. In general, N deficiency promotes root growth including root length, diameter and volume, and lateral root length depending on soil environment and N distribution [7,27–29,31]. *Lus10024908*, the ortholog of *Arabidopsis* *NAC021* mediates auxin signaling to promote lateral root development, and its overexpression results in a higher number and longer lateral roots [69]. Another interesting DEG involved in lateral root development was *Lus10040592*. Its ortholog in *Arabidopsis* is *SUNN*, which controls lateral root density in response to N concentration through the modulation of shoot-to-root auxin transport [75]. Lateral roots are organs that are under the control of nutrient supply such as N or phosphate, and modification of their architecture is a key mechanism underlying plant response to nutrient depleted soil conditions [65,75]. For example, *Lus10011346*, the ortholog of *WRKY75* transcription factor, mediates phosphate acquisition and lateral root development in *Arabidopsis* [65]. Most of the DEGs involved in root development were downregulated in the LN genotype, in agreement with its 36.3, 46.8 and 36.1% reductions in TRL, RV and RT, respectively, under N– compared to the HN genotype. Taken together, the root transcriptome analysis provided a valuable catalog of DEGs, which further support the negative effects of N stress on biomass production, root architecture, N content in roots



and shoots, energy production and ultimately NUE, as witnessed in *Brassica juncea* [107], *Solanum tuberosum* [104] and *Brassica napus* [31].

### 3.5. Differentially Expressed Genes at QTLs

Omics research is now shifting from single-omics to large-scale multi-omics approaches [108]. Through this approach, an understanding of the fundamental biological processes can be achieved for a more accurate prediction of the response variable, and we can gain further insights into the mechanistic aspects of the system [108]. Through the multi-omics approach, researchers can obtain a deeper understanding of the fundamental biological processes, attain more accurate predictions for the response variables and gain further insights into the mechanistic aspects of the system [108]. Combining GWAS with RNA-seq improves the accuracy of candidate gene selection [109]. For example, eight salt stress-related candidate genes were identified by a combination of GWAS and transcriptome analysis in *Medicago sativa* (lucerne) [110]. Through the integration of GWAS and RNA-seq, fourteen candidate genes responsive to drought stress were identified in *Helianthus annuus* (common sunflower) [109]. Similarly, combining QTL mapping, GWAS and transcriptome analysis enabled the identification of genes involved in high-temperature stress tolerance in *Oryza sativa* (rice) [111]. Here, the root RNA-seq analysis allowed us to locate 337 DEGs in 169 QTLs (47.1%), to identify DEGs in NUE-related QTLs and to confirm the robustness of the mathematical algorithms upon which ML-GWAS analyses rely.

Both carbon (C) and N nutrients are essential for various cellular functions, and therefore adequate supply of these two nutrients is critical for plant growth and stress response. *CBL-interacting serine/threonine-protein kinase 14* (*CIPK14*, *Lus10022748*) has been shown to coordinate the responses to oxygen and sugar deficiencies in rice and coordinate the C and N signaling pathways in response to the relative C/N status in rice seedling roots [51]. *CIPK14*, located in QTL Lu1\_9831112 and associated with TRL\_Index, was upregulated in the LN genotype. Similarly, *Gamma-glutamylcyclotransferase 2.1* (*GGCT2.1*, *Lus10020181*) catalyzes the formation of 5-oxoproline from gamma-glutamyl dipeptides and plays a significant role in glutathione (GSH) homeostasis. In *Arabidopsis*, *GGCT2.1* mobilizes L-cysteine from glutathione when there is insufficient sulfate for de novo L-cysteine synthesis, and under sulfur-starvation, induces changes in the root system architecture through activity of the gamma-glutamyl cycle in the primary root tip [79]. In our study, QTL Lu2\_4220131 was found to be associated with the RT\_Index, and carried the up-regulated *GGCT2.1* gene, which was up-regulated under N<sup>-</sup>, suggesting that both sulfur and N starvation could initiate the same glutathione degradation mechanism to produce the component amino acids L-glutamate, L-cysteine and L-glycine. More than 50 distinct amino acid transporter genes have been identified in the *Arabidopsis* genome, indicating that the movement of amino acids across membranes is a highly complex process in plants. The *Arabidopsis* ortholog *cationic amino acid transporter 8* (*CAT8*, *Lus10005574*) located in QTL Lu14\_17132252 (R/S\_N+) is involved in the movement of the cationic neutral or acidic amino acids and is preferentially expressed in young and rapidly dividing tissues such as young leaves and root apical meristem [78]. Thus, *CAT8* may be involved in allocation of the amino acids' glutamine and glutamic acid to root and shoot meristems as precursors for the synthesis of other amino acids under N<sup>-</sup> [78].

In plants that have been deprived of nitrate for a significant length of time, a constitutive high-affinity nitrate transport system was shown to be responsible for initial nitrate uptake [59]. *Arabidopsis high affinity nitrate transporter 2.5* (*NRT2.5*, *Lus10030902*) included within the LD block of QTL Lu13\_18439316 (RT\_Index, R/S\_N+) is predominantly expressed in roots of nitrate-deprived plants as a 150 kDa molecular complex with *NRT3.1*. This complex accounts for 63% of the constitutive high-affinity nitrate transport system influx and is the major contributor to nitrate absorption [59].

Root development and root architecture plasticity are pivotal processes in N stress responses. In *Arabidopsis*, ethylene is biosynthesized from S-adenosyl-L-methionine through *1-aminocyclopropane-1-carboxylate oxidase 1* (*ACO1*, *Lus10008564*). In flax, *ACO1*, located in

QTL Lu11\_14898826 (NUE\_N<sup>-</sup>), could play a regulatory role in lateral root development, as in *Arabidopsis* where *aco1* mutants showed reduced ethylene production in root tips compared to wild-type and displayed altered lateral root formation [62]. *LRR receptor-like serine/threonine-protein kinase GSO1* (*GSO1*, *Lus10036251*) in coordination with *GSO2*, regulates seedling root growth through control of cell division and cell fate specification [63]. *GSO1*, a DEG located in QTL Lu12\_1386203 and associated with RT\_N<sup>+</sup> and R/S\_N<sup>-</sup>, is a prime candidate considering its role in root development.

Together, the DEGs identified at QTLs and their important and well documented roles in N metabolism, root development, energy production, amino acid transport/catabolism and diverse abiotic stresses demonstrate the efficacy of combining omics tools for rapid identification of candidate genes controlling complex traits like NUE and other related abiotic stresses [31,35,109].

### 3.6. GWAS-Assisted Genomic Selection

Genomic selection (GS) is a promising approach used in crop breeding programs, particularly for improving complex traits. In GS, genome-wide markers are used to predict the genomic-estimated breeding values (GEBVs) of individuals by capturing the benefits of both major- and minor-effect QTLs [36]. By replacing the phenotypic selection with the GEBV, the genetic gain for each unit cycle can be increased [112]. GS reduced the selection cycle length of maize, *Arabidopsis* and barley breeding programs compared to phenotypic selection that otherwise could take several cycles of extensive phenotyping to develop reliable phenotypic data [113]. However, performing GS using a large number of markers is challenging, due to the curse of dimensionality as well as multicollinearity arising from LD between markers [114]. In addition, molecular markers are major factors affecting both genomic prediction accuracy ( $r$ ) and the cost of GS [41]. Previous studies have indicated that the use of QTLs as markers in GS significantly increases prediction accuracy compared with genome-wide random markers [41,95,101]. This approach, also known as GWAS-assisted GS, produced a superior prediction accuracy of 0.92 when 500 QTLs associated with pasmo resistance were used compared to an accuracy of 0.67 when 52,347 random SNPs were employed in the GS models in flax [95]. Similarly, the GWAS-assisted GS strategy outperformed the prediction accuracies obtained with 17,277 genome-wide SNPs for seven breeding selection traits in flax including yield, days to maturity, iodine value, seed protein content, oil content, linoleic acid and linolenic acid contents [41]. Here, we compared GBLUP GS models to predict NUE\_STI using five marker sets including a random genome-wide marker set (M1 = 16,383 SNPs) and four GWAS-QTL-based marker sets (M2-M5). Our results confirmed the superiority of all GWAS-based marker sets for GS in NUE\_STI ( $r = 0.62$  to  $0.79$ ) over the random genome-wide marker set ( $r = 0.11$ ), as previously reported in flax [41,95,101] and maize [115]. Interestingly, the highest prediction accuracy for NUE\_STI ( $r = 0.79$ ) was observed when the smallest marker dataset of only 16 trait-specific QTLs was used. Because pleiotropy suggests that different traits might be genetically controlled by the same or tightly linked genes/QTLs, we hypothesized that traits correlated with NUE\_STI are genetically controlled by pleiotropic QTLs that can be used as markers in GS to improve prediction accuracy. Our results rejected the hypothesis, indicating that QTLs from correlated traits did not overcome GS accuracy as compared with trait-specific QTLs, but was the second-best model. This outcome might be caused by QTLs' redundancy or background noise as observed for seven breeding selection traits in flax [41] and should be evaluated on a case-by-case basis, depending on the trait and its correlated contributing traits. Hence, our results suggest that trait-specific QTLs not only significantly improved prediction accuracy, but also reduced the number of markers, which in turn would decrease genotyping cost in practical breeding programs [41,101]. However, as we used as validating population different partitioning of the same 123 accessions, a potential confounding effect was observed as artificial inflation of the predictive ability might occur for the QTL data sets. As a recommendation to minimize artificial inflation, the best GS model should be tested in an independent set of genotypes [116].

Another important factor determining higher prediction accuracy is the size of the training population and its genetic diversity. In flax, using different training population sizes derived from the Canadian flax core collection ( $n = 370$ ), the prediction accuracies for pasmo resistance ranged from 0.8 with 50 genotypes to 0.9 with 185 accessions, whereas smaller accuracy gains up to 0.93 were obtained between 200 and 370 individuals [95]. Here, we used a training population of 123 diverse individuals, which, based on previous reports, is expected to provide sufficient genetic diversity and, therefore, abundant favorable QTL alleles for NUE-related traits useful to construct robust GS models [35,87,95]. Despite the prediction accuracy for NUE\_STI being the highest when the GBLUP model was performed with the 16 trait-specific QTLs marker set, the evaluation of additional parametric and non-parametric GS models could improve  $r$  values for NUE\_STI, as observed for maize [115] and wheat [116]. However, the highest prediction accuracies not only depend on the GS model, but also on the genetic architecture of the target trait, the extent of LD, and the genetic diversity of the training population, factors that should be addressed before implementing practical breeding programs.

#### 4. Materials and Methods

##### 4.1. Plant Materials

An association panel consisted of 123 flax accessions and representing the genetic diversity from 28 countries was assembled from the Canadian flax core collection [86]. The plant materials include 83 cultivars, 21 breeding lines, 5 landraces and 14 accessions of unknown improvement status grouped into 88 oilseed and 35 fiber morphotypes (Table S1).

##### 4.2. Plant Growth Conditions and Phenotyping

Seeds from each of the 123 flax accessions were germinated in Petri dishes on filter paper wet with distilled water. After seven days, two uniform seedlings were transplanted into pots ( $648 \text{ cm}^3$ ) filled with sterile silver sand. Seedlings were watered daily with 30 mL of modified Hoagland's nutrient solution. Briefly, the nutrient solution contained 2.5 mM  $\text{K}_2\text{SO}_4$ , 2 mM  $\text{MgSO}_4$ , 1 mM  $\text{KH}_2\text{PO}_4$ , 1 mL  $\text{L}^{-1}$  Hoagland micronutrients and 2 mL  $\text{L}^{-1}$  FeEDTA solution [12]. Two treatments were evaluated with nitrate added to the solution in the form of 500 mM  $\text{Ca}(\text{NO}_3)_2$ , to obtain  $\text{NO}_3^-$  concentrations of 2.5 mM, referred to as N+ or (0 mM N) referred to as N-. To adjust  $\text{Ca}^{2+}$  concentration to the same values in both N treatments, 0.9 mM  $\text{CaSO}_4$  was added to the N- treatment. Pots were moved to a greenhouse facility maintained at 18–25 °C, with an 18 h day/6 h night photoperiod and 30–50% relative humidity. The photosynthetically active radiation (PAR) was approximately  $400 \mu\text{mol m}^{-2} \text{ s}^{-1}$ . The experiment was laid out as a completely randomized design with three biological replicates, totaling six plants per genotype. After 14 days, pots were immersed in water to loosen the soil and the roots were released. The seedlings from each N treatment and genotype were collected and cut into root and shoot sections. The root system of each plant was imaged using a calibrated optical scanner LA2400 (Epson 11000XL, Long Beach, CA, USA). Root images were analyzed using the WinRHIZO software v.2.0 (Regent Instruments, Montreal, QC, Canada), and the measurement data obtained was used to calculate the following root traits: (i) total root length (TRL; cm), (ii) root volume (RV;  $\text{cm}^3$ ) and (iii) number of root tips (RT). Thereafter, plant tissues were placed in an oven at 60 °C for two days, after which plant dry weight (PDW), root dry weight (RDW), shoot dry weight (SDW) were determined, and root/shoot ratio was calculated. Shoot and root N content were determined using the Dumas combustion method in a Gerhardt, DUMATHERM® N Pro analyzer as described by Muñoz-Huerta [117].

##### 4.3. Phenotypic Data Analysis

Statistical differences between treatments, genotypes and genotype x treatment interactions for shoot and root traits were analyzed using a Restricted Maximum Likelihood (REML) analysis implemented in GenStat v.18 [118] with  $p < 0.05$  as threshold. Best linear unbiased estimates (BLUEs) were obtained for each trait under both N treatments and

used to calculate the trait stability indices using the ratio of the trait under N− to the trait under N+ [119]. NUE values were calculated using the following formula: plant dry weight (mg)/Plant N content (mg). NUE stress tolerance index (NUE\_STI) was estimated according to Fernandez [120]. All traits were used as input for the multi-locus GWAS analyses. Pearson's correlation analyses were conducted using the R package "ggplot2" v.3.4.4 [121] to determine the correlations between the 21 NUE-related traits and their distributions under N− and N+ conditions.

#### 4.4. Genotyping, Genetic Structure and Linkage Disequilibrium

SNP data was generated for the entire flax core collection (n = 407) by resequencing all the accessions using Illumina HiSeq 2000 platform in a 100 bp paired-end mode at an average genome coverage of 17× and generating a data set of 570,443 high-quality SNPs with a call rate > 80%. From this core data set, SNP information was extracted for the above mentioned 123 accessions and further filtered at a call rate > 95% and a minor allele frequency (MAF) > 0.05, and the resulting 272,944 SNP dataset was used for this study.

The genetic structure of the 123 accessions was evaluated in STRUCTURE v.2.3.4 [122] using a subset of 5305 SNPs generated from the 272,944 SNP dataset at a call rate > 98% and a MAF > 0.05 and that were found evenly distributed across the 15 pseudomolecules of flax [48]. The number of sub-groups was determined using the web-based software Structure Harvester v.0.6.94 (<http://taylor0.biology.ucla.edu/structureHarvester/>, (accessed on 14 July 2023)), which is based on the Evanno method [123]. Neighbor-joining (NJ) phylogenetic, principal component (PC) and kinship analyses were performed based on the 272,944 SNPs using TASSEL v 5.2.31 [124].

Genome-wide and chromosome-specific linkage disequilibrium (LD) were estimated using the squared correlations of allele frequency ( $r^2$ ) in TASSEL v.5.2.31 [124] with a sliding window size of 50. LD decay was estimated as previously described by Soto-Cerda [94].

#### 4.5. Multi-Locus Genome-Wide Association Analyses

To identify the genetic loci underlying NUE-related traits, the ML-GWAS methods FASTmrEMMA [125], FASTmrMLM [126], ISIS EM-BLASSO [127], mrMLM [128], pKwMEB [129] and pLARMEB [130] included in the R package multi-locus random-SNP-effect mixed linear model (mrMLM v. 4.0.2) [131], were computed using the default parameters. A logarithm of the odds (LOD) score > 3.0 was set as threshold to detect robust marker-trait associations, which increases the QTN detection power compared to single-locus GWAS while reducing type I errors [125–130]. The ML-GWAS outcomes were summarized and displayed using Manhattan plots, and their ability to minimize false-positive associations was tested with quantile–quantile (Q-Q) plots. The mrMLM v. 4.0.2 package constructs the Manhattan and Q-Q plots using the  $-\log_{10}(p)$  median among the  $-\log_{10}(p)$  values of each marker obtained from the mrMLM, FASTmrMLM, FASTmrEMMA and pKwMEB models. Irrespective of the  $-\log_{10}(p)$  median, only significant markers (LOD > 3.0) are therefore shown in the Manhattan plots above dotted vertical lines [131].

Significant QTNs detected by the ML-GWAS analyses were further filtered using the Mann–Whitney non-parametric U test ( $p < 0.05$ ). QTNs with non-significant allele effect were considered false positives and were removed. The QTNs with significant allele effect were grouped into QTL blocks if they belonged to a physical distance corresponding to 75% of the maximum LD decay. As such, neighboring QTNs within QTL blocks had a high probability of remaining linked across generations [132]. For each QTL block, the QTN with the largest % of phenotypic variations explained ( $R^2$ ) value was selected as the representative QTN for the QTL block. Boxplots to visualize QTL allele effect were made using the R package "ggplot2" [121]. Adjusted  $R^2$  ( $\text{adj}R^2$ ) values for all QTL associated with NUE-related traits were calculated based on simple regressions of QTL on traits because the  $\text{adj}R^2$  values represent the proportion of the total variation of traits explained by the QTL [95].



The simple regression analyses were conducted using Blue Sky statistics (<https://www.blueskystatistics.com/>) (accessed on 10 May 2023).

#### 4.6. Transcriptome Sequencing and Analysis

From the N stress experiment described above, two contrasting flax accessions O\_IRL\_C\_CN98192 and O\_IND\_C\_CN98982, referred to as high NUE (HN) and low NUE (LN) hereafter, respectively, were selected and submitted again to the same N stress experiment using the modified Hoagland's nutrient solution as described above. Root samples were collected 14 days after transplanting and immediately frozen in liquid nitrogen. The experiment included four biological replicates per genotype and treatment (N<sup>-</sup> and N<sup>+</sup>), for a total of 16 experimental units. Total RNA was extracted from the root tissue of each of the 16 biological sample units using the Spectrum Plant Total RNA kit (Sigma-Aldrich, St. Louis, MO, USA). RNA was DNase-treated, visualized on an agarose gel, quantified using a Nanodrop (Thermo Scientific, Madison, WI, USA) and RNA QC for all samples was ensured by RNA integrity number (RIN)  $\geq 7.0$  using a 2100 Bioanalyzer (Agilent Technologies, Santa Clara, CA, USA). The 16 RNA libraries were constructed by outsourcing to Novogene Corporation Inc. (Beijing, China) and were sequenced in paired-end mode using a NovaSeq 6000 platform (Illumina, Inc., San Diego, CA, USA) through 150 cycles. The sequencing results in FASTQ format were processed with Trimmomatic v.1 [133] which involved the removal of bases with a q-score below 15 from both their 5' and 3' ends, while retaining sequences that were longer than 70 base pairs. The high-quality reads were mapped to the flax reference genome [48] using HISAT2 v2.2.1 [134] with default parameters. The alignment bam files were processed and sorted with samtools v1.3.1 [135] and the abundance of genomic features was computed using featureCounts v2.0.1 [136]. The statistical differences in gene expression were assessed with the R package DESeq2 [137] with the threshold set as  $|\log_2(\text{Fold change})| \geq 1$  and false discovery rate (FDR)-adjusted  $p$  value  $< 0.05$ .

Functional annotation of the DEGs was carried out against the curated KEGG GENES database using the KEGG Automatic Annotation Server (KAAS, <https://www.genome.jp/kegg/>) (accessed on 12 January 2023). KEGG Orthologs (KO) were assigned using the KofamKOALA software [138].

#### 4.7. Cross-Referencing of Differentially Expressed Genes and QTL-Associated Candidate Genes

GWAS-detected QTL were scanned within an estimated average genome-wide LD decay range of 100 kb (Figure 2d) for the identification of candidate genes mined from the flax reference genome [48] using the Jbrowse feature of Phytozome v.13.1 (<http://phytozome.jgi.doe.gov/pz/portal.html>) (accessed on 13 January 2023).

Candidate genes identified near the QTL were further analyzed and cross-referenced with the root RNA-seq transcriptomic data from the two contrasting flax accessions HN and LN for their involvement in nitrogen stress responses. Only DEGs with a fold change  $\geq 1$  and an FDR-adjusted  $p$  value  $< 0.05$  were considered for cross-referencing with candidate genes associated with the QTL. To determine the biological significance of the DEGs, *L. usitatissimum* genes were annotated by BLASTP against the SwissProt database using the threshold criteria of identity  $\geq 50\%$ , sequence coverage  $\geq 70\%$  and E-value  $\leq 1 \times e^{-10}$ . The functional role of DEGs in nitrogen stress responses were further examined by searching literature reports for their functional characterization in other plant species.

#### 4.8. GWAS-Assisted Genomic Selection

Markers (QTLs) obtained from the ML-GWAS were used to predict the GEBV of NUE\_STI, a trait that allows the identification of genotypes with high NUE and high N responses. Five marker sets were tested as GS input. Marker set 1 (M1) was constructed using 16,383 random genome-wide markers; marker set 2 (M2) considered the markers identified by GWAS to be associated with all traits under the N<sup>-</sup> conditions ( $n = 120$ ); marker set 3 (M3) included only the markers associated with NUE\_STI ( $n = 16$ ); marker set

4 (M4) was constructed with the markers associated with all traits positively correlated with NUE\_STI (n = 281); and marker set 5 (M5) was assembled using the markers associated with all traits positively correlated with NUE\_STI that harbored DEGs (n = 127). The goal was to determine the best dataset to obtain the highest prediction accuracy for NUE\_STI, considering QTL identified for NUE\_STI per se, and those of traits correlated with it [139].

The genomic BLUP (GBLUP) statistical model, implemented in the R package BGLR (<https://r-forge.r-project.org/projects/bglr/>, accessed on 12 January 2023) [140], was used to evaluate prediction accuracy of the five marker sets because GBLUP's superior prediction ability for highly polygenic traits has been demonstrated in flax [41,101]. The computation methodology of GBLUP has been previously described in more detail by De Los Campos [141]. The marker sets were formatted as "1" for the positive effect allele of a QTL and "−1" for the alternative allele [95].

For GS model validation, a fivefold random cross-validation strategy was applied [95]. The 123 accessions were randomly partitioned into five subsets. For a given partition, each subset was used as test data, whereas the remaining four subsets were used as a training dataset. This partitioning was repeated 100 times. The accuracy of GS (r) was computed using the Pearson's correlation coefficient between the genetic values predicted by GS and the observed phenotypic values. To compare the different marker sets, an analysis of variance (ANOVA) with Tukey's multiple pairwise comparisons was conducted to determine the statistical significance of differences in genomic prediction (r) using GenStat v18 [118] with  $p < 0.05$ . Boxplots for each marker set were made using the R package "ggplot2" [121].

## 5. Conclusions

The 123 flax accessions exhibited abundant genetic diversity for NUE-related traits, in line with their diverse geographic origin, breeding status and plant morphotype, resulting in the identification of 359 NUE-related trait QTLs. This study reaffirmed the polygenic nature of NUE and its related traits which are controlled by many small and medium effect QTLs in flax. Root RNA-seq analysis identified important candidate genes involved in root development and N metabolism, among which 337 candidates were found at 169 QTLs. GWAS-assisted GS strategy produced superior genomic prediction accuracies compared to genome-wide markers for NUE\_STI, and the GS model based on trait-specific QTLs had the best predictive ability (r = 0.79). The use of GWAS-derived QTL associated with a target trait is recommended because it is the most accurate, cost-effective and computationally advantageous for NUE and other quantitative traits in flax.

**Supplementary Materials:** The following supporting information can be downloaded at: <https://www.mdpi.com/article/10.3390/ijms242417624/s1>.

**Author Contributions:** Conceptualization, S.C.; Formal analysis, G.L. and G.A.; Funding acquisition, B.J.S.-C.; Writing—original draft, B.J.S.-C. and G.L.; Writing—review and editing, S.C., B.F. and C.I.-B. All authors have read and agreed to the published version of the manuscript.

**Funding:** This work was funded by Fondo Nacional de Desarrollo Científico y Tecnológico (FONDECYT) project No. 1200241. Universidad Católica de Temuco acknowledges the collaboration of Agriculture and Agri-Food Canada (AAFC) and the Total Utilization Flax GENomics (TUFGEN) project formerly funded by Genome Canada and other stakeholders of the Canadian flax industry.

**Data Availability Statement:** The raw RNA-seq data were deposited in the NCBI under the bio-project PRJNA921700 (<https://www.ncbi.nlm.nih.gov/bioproject/PRJNA921700> (accessed on 7 January 2023)).

**Acknowledgments:** The authors also acknowledge the supercomputing infrastructure of Soroban (SATREPS MACH—JPM/JSA1705) at Centro de Modelación y Computación Científica at Universidad de La Frontera.

**Conflicts of Interest:** The authors declare no conflict of interest.

## References

1. Qin, L.; Walk, T.C.; Han, P.; Chen, L.; Zhang, S.; Li, Y.; Hu, X.; Xie, L.; Yang, Y.; Liu, J.; et al. Adaption of Roots to Nitrogen Deficiency Revealed by 3D Quantification and Proteomic Analysis. *Plant Physiol.* **2019**, *179*, 329–347. [[CrossRef](#)] [[PubMed](#)]
2. Shrawat, A.K.; Carroll, R.T.; DePauw, M.; Taylor, G.J.; Good, A.G. Genetic Engineering of Improved Nitrogen Use Efficiency in Rice by the Tissue-Specific Expression of Alanine Aminotransferase. *Plant Biotechnol. J.* **2008**, *6*, 722–732. [[CrossRef](#)] [[PubMed](#)]
3. UNEP. *Frontiers 2018/2019 Emerging Issues of Environmental Concern*; United Nations Environment Programme: Nairobi, Kenya, 2019.
4. Lei, L.; Li, G.; Zhang, H.; Powers, C.; Fang, T.; Chen, Y.; Wang, S.; Zhu, X.; Carver, B.F.; Yan, L. Nitrogen Use Efficiency Is Regulated by Interacting Proteins Relevant to Development in Wheat. *Plant Biotechnol. J.* **2018**, *16*, 1214–1226. [[CrossRef](#)] [[PubMed](#)]
5. Billen, G.; Garnier, J.; Lassaletta, L. The Nitrogen Cascade from Agricultural Soils to the Sea: Modelling Nitrogen Transfers at Regional Watershed and Global Scales. *Philos. Trans. R. Soc. B Biol. Sci.* **2013**, *368*, 20130123. [[CrossRef](#)] [[PubMed](#)]
6. Gruber, N.; Galloway, J.N. An Earth-System Perspective of the Global Nitrogen Cycle. *Nature* **2008**, *451*, 293–296. [[CrossRef](#)] [[PubMed](#)]
7. Bouchet, A.S.; Laperche, A.; Bissuel-Belaygue, C.; Snowdon, R.; Nesi, N.; Stahl, A. Nitrogen Use Efficiency in Rapeseed. A Review. *Agron. Sustain. Dev.* **2016**, *36*, 38. [[CrossRef](#)]
8. Moll, R.H.; Kamprath, E.J.; Jackson, W.A. Analysis and Interpretation of Factors Which Contribute to Efficiency of Nitrogen Utilization. *Agron. J.* **1982**, *74*, 562–564. [[CrossRef](#)]
9. Masclaux-Daubresse, C.; Daniel-Vedele, F.; Dechorgnat, J.; Chardon, F.; Gaufichon, L.; Suzuki, A. Nitrogen Uptake, Assimilation and Remobilization in Plants: Challenges for Sustainable and Productive Agriculture. *Ann. Bot.* **2010**, *105*, 1141–1157. [[CrossRef](#)]
10. Li, P.; Chen, F.; Cai, H.; Liu, J.; Pan, Q.; Liu, Z.; Gu, R.; Mi, G.; Zhang, F.; Yuan, L. A Genetic Relationship between Nitrogen Use Efficiency and Seedling Root Traits in Maize as Revealed by QTL Analysis. *J. Exp. Bot.* **2015**, *66*, 3175–3188. [[CrossRef](#)]
11. Kant, S.; Bi, Y.M.; Rothstein, S.J. Understanding Plant Response to Nitrogen Limitation for the Improvement of Crop Nitrogen Use Efficiency. *J. Exp. Bot.* **2011**, *62*, 1499–1509. [[CrossRef](#)]
12. Abenavoli, M.R.; Longo, C.; Lupini, A.; Miller, A.J.; Araniti, F.; Mercati, F.; Princi, M.P.; Sunseri, F. Phenotyping Two Tomato Genotypes with Different Nitrogen Use Efficiency. *Plant Physiol. Biochem.* **2016**, *107*, 21–32. [[CrossRef](#)] [[PubMed](#)]
13. Luo, L.; Zhang, Y.; Xu, G. How Does Nitrogen Shape Plant Architecture? *J. Exp. Bot.* **2020**, *71*, 4415–4427. [[CrossRef](#)] [[PubMed](#)]
14. Lérán, S.; Muñoz, S.; Brachet, C.; Tillard, P.; Gojon, A.; Lacombe, B. Arabidopsis NRT1.1 Is a Bidirectional Transporter Involved in Root-to-Shoot Nitrate Translocation. *Mol. Plant* **2013**, *6*, 1984–1987. [[CrossRef](#)] [[PubMed](#)]
15. Kanno, Y.; Hanada, A.; Chiba, Y.; Ichikawa, T.; Nakazawa, M.; Matsui, M.; Koshiha, T.; Kamiya, Y.; Seo, M. Identification of an Abscisic Acid Transporter by Functional Screening Using the Receptor Complex as a Sensor. *Proc. Natl. Acad. Sci. USA* **2012**, *109*, 9653–9658. [[CrossRef](#)] [[PubMed](#)]
16. Li, J.Y.; Fu, Y.L.; Pike, S.M.; Bao, J.; Tian, W.; Zhang, Y.; Chen, C.Z.; Zhang, Y.; Li, H.M.; Huang, J.; et al. The Arabidopsis Nitrate Transporter NRT1.8 Functions in Nitrate Removal from the Xylem Sap and Mediates Cadmium Tolerance. *Plant Cell* **2010**, *22*, 1633–1646. [[CrossRef](#)] [[PubMed](#)]
17. Wang, Y.Y.; Tsay, Y.F. Arabidopsis Nitrate Transporter NRT1.9 Is Important in Phloem Nitrate Transport. *Plant Cell* **2011**, *23*, 1945–1957. [[CrossRef](#)] [[PubMed](#)]
18. Hsu, P.K.; Tsay, Y.F. Two Phloem Nitrate Transporters, NRT1.11 and NRT1.12, Are Important for Redistributing Xylem-Borne Nitrate to Enhance Plant Growth. *Plant Physiol.* **2013**, *163*, 844–856. [[CrossRef](#)] [[PubMed](#)]
19. Li, H.; Hu, B.; Chu, C. Nitrogen Use Efficiency in Crops: Lessons from Arabidopsis and Rice. *J. Exp. Bot.* **2017**, *68*, 2477–2488. [[CrossRef](#)]
20. Hudson, D.; Guevara, D.; Yaish, M.W.; Hannam, C.; Long, N.; Clarke, J.D.; Bi, Y.M.; Rothstein, S.J. GNC and CGA1 Modulate Chlorophyll Biosynthesis and Glutamate Synthase (GLU1/FD-GOGAT) Expression in Arabidopsis. *PLoS ONE* **2011**, *6*, e26765. [[CrossRef](#)]
21. Alvarez, J.M.; Riveras, E.; Vidal, E.A.; Gras, D.E.; Contreras-López, O.; Tamayo, K.P.; Aceituno, F.; Gómez, I.; Ruffel, S.; Lejay, L.; et al. Systems Approach Identifies TGA1 and TGA4 Transcription Factors as Important Regulatory Components of the Nitrate Response of Arabidopsis Thaliana Roots. *Plant J.* **2014**, *80*, 1–13. [[CrossRef](#)]
22. Garnett, T.; Plett, D.; Heuer, S.; Okamoto, M. Genetic Approaches to Enhancing Nitrogen-Use Efficiency (NUE) in Cereals: Challenges and Future Directions. *Funct. Plant Biol.* **2015**, *42*, 921–941. [[CrossRef](#)]
23. Cormier, F.; Foulkes, J.; Hirel, B.; Gouache, D.; Moënné-Loccoz, Y.; Le Gouis, J. Breeding for Increased Nitrogen-Use Efficiency: A Review for Wheat (*T. aestivum* L.). *Plant Breed.* **2016**, *135*, 255–278. [[CrossRef](#)]
24. Plett, D.; Garnett, T.; Okamoto, M. Molecular Genetics to Discover and Improve Nitrogen Use Efficiency in Crop Plants. In *Plant Macronutrient Use Efficiency: Molecular and Genomic Perspectives in Crop Plants*; Elsevier: Amsterdam, The Netherlands, 2017; pp. 93–122. ISBN 9780128113080.
25. Hirel, B.; Bertin, P.; Quilleré, I.; Bourdoncle, W.; Attagnant, C.; Dellay, C.; Gouy, A.; Cadiou, S.; Retailiau, C.; Falque, M.; et al. Towards a Better Understanding of the Genetic and Physiological Basis for Nitrogen Use Efficiency in Maize. *Plant Physiol.* **2001**, *125*, 1258–1270. [[CrossRef](#)]
26. Kang, Y.; Sakiroglu, M.; Krom, N.; Stanton-Geddes, J.; Wang, M.; Lee, Y.C.; Young, N.D.; Udvardi, M. Genome-Wide Association of Drought-Related and Biomass Traits with HapMap SNPs in Medicago Truncatula. *Plant Cell Environ.* **2015**, *38*, 1997–2011. [[CrossRef](#)]

27. Cormier, F.; Le Gouis, J.; Dubreuil, P.; Lafarge, S.; Praud, S. A Genome-Wide Identification of Chromosomal Regions Determining Nitrogen Use Efficiency Components in Wheat (*Triticum aestivum* L.). *Theor. Appl. Genet.* **2014**, *127*, 2679–2693. [[CrossRef](#)]
28. Monostori, I.; Szira, F.; Tondelli, A.; Árendás, T.; Gierczik, K.; Cattivelli, L.; Galiba, G.; VÁgújfalvi, A. Genome-Wide Association Study and Genetic Diversity Analysis on Nitrogen Use Efficiency in a Central European Winter Wheat (*Triticum aestivum* L.) Collection. *PLoS ONE* **2017**, *12*, e0189265. [[CrossRef](#)]
29. Morosini, J.S.; Mendonça, L.d.F.; Lyra, D.H.; Galli, G.; Vidotti, M.S.; Fritsche-Neto, R. Association Mapping for Traits Related to Nitrogen Use Efficiency in Tropical Maize Lines under Field Conditions. *Plant Soil* **2017**, *421*, 453–463. [[CrossRef](#)]
30. Gupta, N.; Gupta, M.; Akhatar, J.; Goyal, A.; Kaur, R.; Sharma, S.; Goyal, P.; Mukta, A.; Kaur, N.; Mittal, M.; et al. Association Genetics of the Parameters Related to Nitrogen Use Efficiency in *Brassica juncea* L. *Plant Mol. Biol.* **2021**, *105*, 161–175. [[CrossRef](#)]
31. Ahmad, N.; Su, B.; Ibrahim, S.; Kuang, L.; Tian, Z.; Wang, X.; Wang, H.; Dun, X. Deciphering the Genetic Basis of Root and Biomass Traits in Rapeseed (*Brassica napus* L.) through the Integration of GWAS and RNA-Seq under Nitrogen Stress. *Int. J. Mol. Sci.* **2022**, *23*, 7958. [[CrossRef](#)] [[PubMed](#)]
32. Guo, J.; Li, C.; Zhang, X.; Li, Y.; Zhang, D.; Shi, Y.; Song, Y.; Li, Y.; Yang, D.; Wang, T. Transcriptome and GWAS Analyses Reveal Candidate Gene for Seminal Root Length of Maize Seedlings under Drought Stress. *Plant Sci.* **2020**, *292*, 110380. [[CrossRef](#)] [[PubMed](#)]
33. Wang, W.; Wang, L.; Wang, L.; Tan, M.; Ogutu, C.O.; Yin, Z.; Zhou, J.; Wang, J.; Wang, L.; Yan, X. Transcriptome Analysis and Molecular Mechanism of Linseed (*Linum usitatissimum* L.) Drought Tolerance under Repeated Drought Using Single-Molecule Long-Read Sequencing. *BMC Genom.* **2021**, *22*, 109. [[CrossRef](#)] [[PubMed](#)]
34. Liu, H.; Li, X.; Zhang, Q.; Yuan, P.; Liu, L.; King, G.J.; Ding, G.; Wang, S.; Cai, H.; Wang, C.; et al. Integrating a Genome-Wide Association Study with Transcriptomic Data to Predict Candidate Genes and Favourable Haplotypes Influencing *Brassica napus* Seed Phytate. *DNA Res.* **2021**, *28*, dsab011. [[CrossRef](#)] [[PubMed](#)]
35. Soto-Cerda, B.J.; Larama, G.; Gajardo, H.; Inostroza-Blancheteau, C.; Cloutier, S.; Fofana, B.; Abanto, M.; Aravena, G. Integrating Multi-Locus Genome-Wide Association Studies with Transcriptomic Data to Identify Genetic Loci Underlying Adult Root Trait Responses to Drought Stress in Flax (*Linum usitatissimum* L.). *Environ. Exp. Bot.* **2022**, *202*, 105019. [[CrossRef](#)]
36. Meuwissen, T.H.E.; Hayes, B.J.; Goddard, M.E. Prediction of Total Genetic Value Using Genome-Wide Dense Marker Maps. *Genetics* **2001**, *157*, 1819–1829. [[CrossRef](#)] [[PubMed](#)]
37. Wang, X.; Xu, Y.; Hu, Z.; Xu, C. Genomic Selection Methods for Crop Improvement: Current Status and Prospects. *Crop. J.* **2018**, *6*, 330–340. [[CrossRef](#)]
38. Yu, J.; Pressoir, G.; Briggs, W.H.; Bi, I.V.; Yamasaki, M.; Doebley, J.F.; McMullen, M.D.; Gaut, B.S.; Nielsen, D.M.; Holland, J.B.; et al. A Unified Mixed-Model Method for Association Mapping That Accounts for Multiple Levels of Relatedness. *Nat. Genet.* **2006**, *38*, 203–208. [[CrossRef](#)]
39. Spindel, J.E.; Begum, H.; Akdemir, D.; Collard, B.; Redoña, E.; Jannink, J.L.; McCouch, S. Genome-Wide Prediction Models That Incorporate de Novo GWAS Are a Powerful New Tool for Tropical Rice Improvement. *Heredity* **2016**, *116*, 395–408. [[CrossRef](#)]
40. Minamikawa, M.F.; Nonaka, K.; Kaminuma, E.; Kajiya-Kanegae, H.; Onogi, A.; Goto, S.; Yoshioka, T.; Imai, A.; Hamada, H.; Hayashi, T.; et al. Genome-Wide Association Study and Genomic Prediction in Citrus: Potential of Genomics-Assisted Breeding for Fruit Quality Traits. *Sci. Rep.* **2017**, *7*, 4721. [[CrossRef](#)]
41. Lan, S.; Zheng, C.; Hauck, K.; McCausland, M.; Duguid, S.D.; Booker, H.M.; Cloutier, S.; You, F.M. Genomic Prediction Accuracy of Seven Breeding Selection Traits Improved by QTL Identification in Flax. *Int. J. Mol. Sci.* **2020**, *21*, 1577. [[CrossRef](#)]
42. He, H.; Yang, R.; Li, Y.; Ma, A.; Cao, L.; Wu, X.; Chen, B.; Tian, H.; Gao, Y. Genotypic Variation in Nitrogen Utilization Efficiency of Oilseed Rape (*Brassica napus*) under Contrasting N Supply in Pot and Field Experiments. *Front. Plant Sci.* **2017**, *8*, 1825. [[CrossRef](#)]
43. Dash, P.K.; Cao, Y.; Jailani, A.K.; Gupta, P.; Venglat, P.; Xiang, D.; Rai, R.; Sharma, R.; Thirunavukkarasu, N.; Abdin, M.Z.; et al. Genome-Wide Analysis of Drought Induced Gene Expression Changes in Flax (*Linum usitatissimum*). *GM Crop. Food* **2014**, *5*, 106–119. [[CrossRef](#)]
44. Rabetafika, H.N.; Van Remoortel, V.; Danthine, S.; Paquot, M.; Blecker, C. Flaxseed Proteins: Food Uses and Health Benefits. *Int. J. Food Sci. Technol.* **2011**, *46*, 221–228. [[CrossRef](#)]
45. Soto-Cerda, B.J.; Cloutier, S.; Gajardo, H.A.; Aravena, G.; Quian, R. Identifying Drought-Resilient Flax Genotypes and Related-Candidate Genes Based on Stress Indices, Root Traits and Selective Sweep. *Euphytica* **2019**, *215*, 41. [[CrossRef](#)]
46. Dordas, C.A. Nitrogen Nutrition Index and Its Relationship to N Use Efficiency in Linseed. *Eur. J. Agron.* **2011**, *34*, 124–132. [[CrossRef](#)]
47. Xie, Y.; Gan, Y.; Li, Y.; Niu, J.; Gao, Y.; An, H.; Li, A. Effect of Nitrogen Fertilizer on Nitrogen Accumulation, Translocation, and Use Efficiency in Dryland Oilseed Flax. *Agron. J.* **2015**, *107*, 1931–1939. [[CrossRef](#)]
48. You, F.M.; Xiao, J.; Li, P.; Yao, Z.; Jia, G.; He, L.; Zhu, T.; Luo, M.C.; Wang, X.; Deyholos, M.K.; et al. Chromosome-Scale Pseudomolecules Refined by Optical, Physical and Genetic Maps in Flax. *Plant J.* **2018**, *95*, 371–384. [[CrossRef](#)]
49. Brooks, M.D.; Cirrone, J.; Pasquino, A.V.; Alvarez, J.M.; Swift, J.; Mittal, S.; Juang, C.L.; Varala, K.; Gutiérrez, R.A.; Krouk, G.; et al. Network Walking Charts Transcriptional Dynamics of Nitrogen Signaling by Integrating Validated and Predicted Genome-Wide Interactions. *Nat. Commun.* **2019**, *10*, 1569. [[CrossRef](#)]
50. Xu, N.; Wang, R.; Zhao, L.; Zhang, C.; Li, Z.; Lei, Z.; Liu, F.; Guan, P.; Chu, Z.; Crawford, N.M. The Arabidopsis NRG2 Protein Mediates Nitrate Signaling and Interacts with and Regulates Key Nitrate Regulators. *Plant Cell* **2015**, *28*, 485–504. [[CrossRef](#)] [[PubMed](#)]



51. Hsieh, P.H.; Kan, C.C.; Wu, H.Y.; Yang, H.C.; Hsieh, M.H. Early Molecular Events Associated with Nitrogen Deficiency in Rice Seedling Roots. *Sci. Rep.* **2018**, *8*, 12207. [[CrossRef](#)] [[PubMed](#)]
52. Bouly, J.P.; Gissot, L.; Lessard, P.; Kreis, M.; Thomas, M. Arabidopsis Thaliana Proteins Related to the Yeast SIP and SNF4 Interact with AKIN $\alpha$ 1, an SNF1-like Protein Kinase. *Plant J.* **1999**, *18*, 541–550. [[CrossRef](#)] [[PubMed](#)]
53. Sugiura, M.; Georgescu, M.N.; Takahashi, M. A Nitrite Transporter Associated with Nitrite Uptake by Higher Plant Chloroplasts. *Plant Cell Physiol.* **2007**, *48*, 1022–1035. [[CrossRef](#)] [[PubMed](#)]
54. Wang, R.; Tischner, R.; Gutiérrez, R.A.; Hoffman, M.; Xing, X.; Chen, M.; Coruzzi, G.; Crawford, N.M. Genomic Analysis of the Nitrate Response Using a Nitrate Reductase-Null Mutant of Arabidopsis. *Plant Physiol.* **2004**, *136*, 2512–2522. [[CrossRef](#)] [[PubMed](#)]
55. Sorger, G.; Gooden, D.O.; Earle, E.D.; Mckinnon, J. NADH Nitrate Reductase and NAD(P)H Nitrate Reductase in Genetic Variants and Regenerating Callus of Maize. *Plant Physiol.* **1986**, *82*, 473–478. [[CrossRef](#)] [[PubMed](#)]
56. Funayama, K.; Kojima, S.; Tabuchi-Kobayashi, M.; Sawa, Y.; Nakayama, Y.; Hayakawa, T.; Yamaya, T. Cytosolic Glutamine Synthetase1;2 Is Responsible for the Primary Assimilation of Ammonium in Rice Roots. *Plant Cell Physiol.* **2013**, *54*, 934–943. [[CrossRef](#)]
57. Delay, C.; Imin, N.; Djordjevic, M.A. CEP Genes Regulate Root and Shoot Development in Response to Environmental Cues and Are Specific to Seed Plants. *J. Exp. Bot.* **2013**, *64*, 5383–5394. [[CrossRef](#)] [[PubMed](#)]
58. Remans, T.; Nacry, P.; Pervent, M.; Filleur, S.; Diatloff, E.; Mounier, E.; Tillard, P.; Forde, B.G.; Gojon, A. The Arabidopsis NRT1.1 Transporter Participates in the Signaling Pathway Triggering Root Colonization of Nitrate-Rich Patches. *Proc. Natl. Acad. Sci. USA* **2006**, *103*, 19206–19211. [[CrossRef](#)] [[PubMed](#)]
59. Kotur, Z.; Glass, A.D.M. A 150kDa Plasma Membrane Complex of AtNRT2.5 and AtNAR2.1 Is the Major Contributor to Constitutive High-Affinity Nitrate Influx in Arabidopsis Thaliana. *Plant Cell Environ.* **2015**, *38*, 1490–1502. [[CrossRef](#)]
60. Kanno, Y.; Kamiya, Y.; Seo, M. Nitrate Does Not Compete with Abscisic Acid as a Substrate of AtNPF4.6/NRT1.2/AIT1 in Arabidopsis. *Plant Signal. Behav.* **2013**, *8*, e26624. [[CrossRef](#)]
61. Gazzarrini, S.; Lejay, L.; Gojon, A.; Ninnemann, O.; Frommer, W.B.; Von Wirén, N. Three Functional Transporters for Constitutive, Diurnally Regulated, and Starvation-Induced Uptake of Ammonium into Arabidopsis Roots. *Plant Cell* **1999**, *11*, 937–947. [[CrossRef](#)]
62. Park, C.H.; Roh, J.; Youn, J.H.; Son, S.H.; Park, J.H.; Kim, S.Y.; Kim, T.W.; Kim, S.K. Arabidopsis ACC Oxidase 1 Coordinated by Multiple Signals Mediates Ethylene Biosynthesis and Is Involved in Root Development. *Mol. Cells* **2018**, *41*, 923–932. [[CrossRef](#)]
63. Racolta, A.; Bryan, A.C.; Tax, F.E. The Receptor-like Kinases GSO1 and GSO2 Together Regulate Root Growth in Arabidopsis through Control of Cell Division and Cell Fate Specification. *Dev. Dyn.* **2014**, *243*, 257–278. [[CrossRef](#)] [[PubMed](#)]
64. Seifert, G.J.; Xue, H.; Acet, T. The Arabidopsis Thaliana FASCICLIN LIKE ARABINOGALACTAN PROTEIN 4 Gene Acts Synergistically with Abscisic Acid Signalling to Control Root Growth. *Ann. Bot.* **2014**, *114*, 1125–1133. [[CrossRef](#)] [[PubMed](#)]
65. Devaiah, B.N.; Karthikeyan, A.S.; Raghothama, K.G. WRKY75 Transcription Factor Is a Modulator of Phosphate Acquisition and Root Development in Arabidopsis. *Plant Physiol.* **2007**, *143*, 1789–1801. [[CrossRef](#)]
66. Xue, X.H.; Guo, C.Q.; Du, F.; Lu, Q.L.; Zhang, C.M.; Ren, H.Y. AtFH8 Is Involved in Root Development under Effect of Low-Dose Latrunculin B in Dividing Cells. *Mol. Plant* **2011**, *4*, 264–278. [[CrossRef](#)] [[PubMed](#)]
67. Liberman, L.M.; Sparks, E.E.; Moreno-Risueno, M.A.; Petricka, J.J.; Benfey, P.N. MYB36 Regulates the Transition from Proliferation to Differentiation in the Arabidopsis Root. *Proc. Natl. Acad. Sci. USA* **2015**, *112*, 12099–12104. [[CrossRef](#)] [[PubMed](#)]
68. Van Leene, J.; Blomme, J.; Kulkarni, S.R.; Cannoot, B.; De Winne, N.; Eeckhout, D.; Persiau, G.; Van De Slijke, E.; Vercruyssen, L.; Vanden Bossche, R.; et al. Functional Characterization of the Arabidopsis Transcription Factor BZIP29 Reveals Its Role in Leaf and Root Development. *J. Exp. Bot.* **2016**, *67*, 5825–5840. [[CrossRef](#)] [[PubMed](#)]
69. Xie, Q.; Frugis, G.; Colgan, D.; Chua, N.H. Arabidopsis NAC1 Transduces Auxin Signal Downstream of TIR1 to Promote Lateral Root Development. *Genes Dev.* **2000**, *14*, 3024–3036. [[CrossRef](#)]
70. Moriwaki, T.; Miyazawa, Y.; Kobayashi, A.; Uchida, M.; Watanabe, C.; Fujii, N.; Takahashi, H. Hormonal Regulation of Lateral Root Development in Arabidopsis Modulated by MIZ1 and Requirement of GNOM Activity for MIZ1 Function. *Plant Physiol.* **2011**, *157*, 1209–1220. [[CrossRef](#)]
71. Tabata, R.; Sumida, K.; Yoshii, T.; Ohyama, K.; Shinohara, H.; Matsubayashi, Y. Perception of Root-Derived Peptides by Shoot LRR-RKs Mediates Systemic N-Demand Signaling. *Science* **2014**, *346*, 343–346. [[CrossRef](#)]
72. Shin, R.; Burch, A.Y.; Huppert, K.A.; Tiwari, S.B.; Murphy, A.S.; Guilfoyle, T.J.; Schachtman, D.P. The Arabidopsis Transcription Factor MYB77 Modulates Auxin Signal Transduction. *Plant Cell* **2007**, *19*, 2440–2453. [[CrossRef](#)]
73. Okushima, Y.; Fukaki, H.; Onoda, M.; Theologis, A.; Tasaka, M. ARF7 and ARF19 Regulate Lateral Root Formation via Direct Activation of LBD/ASL Genes in Arabidopsis. *Plant Cell* **2007**, *19*, 118–130. [[CrossRef](#)] [[PubMed](#)]
74. De Smet, I.; Vassileva, V.; De Rybel, B.; Levesque, M.P.; Grunewald, W.; Van Damme, D.; Van Noorden, G.; Naudts, M.; Van Isterdael, G.; De Clercq, R.; et al. Receptor-Like Kinase ACR4 Formative Cell Divisions in the Arabidopsis Root. *Science* **2008**, *322*, 594–597. [[CrossRef](#)] [[PubMed](#)]
75. Jin, J.; Watt, M.; Mathesius, U. The Autoregulation Gene SUNN Mediates Changes in Root Organ Formation in Response to Nitrogen through Alteration of Shoot-to-Root Auxin Transport. *Plant Physiol.* **2012**, *159*, 489–500. [[CrossRef](#)] [[PubMed](#)]
76. Wu, G.; Lewis, D.R.; Spalding, E.P. Mutations in Arabidopsis Multidrug Resistance-Like ABC Transporters Separate the Roles of Acropetal and Basipetal Auxin Transport in Lateral Root Development. *Plant Cell* **2007**, *19*, 1826–1837. [[CrossRef](#)] [[PubMed](#)]



77. Santelia, D.; Vincenzetti, V.; Azzarello, E.; Bovet, L.; Fukao, Y.; Düchtig, P.; Mancuso, S.; Martinoia, E.; Geisler, M. MDR-like ABC Transporter AtPGP4 Is Involved in Auxin-Mediated Lateral Root and Root Hair Development. *FEBS Lett.* **2005**, *579*, 5399–5406. [[CrossRef](#)] [[PubMed](#)]
78. Su, Y.H.; Frommer, W.B.; Ludewig, U. Molecular and Functional Characterization of a Family of Amino Acid Transporters from Arabidopsis. *Plant Physiol.* **2004**, *136*, 3104–3113. [[CrossRef](#)]
79. Joshi, N.C.; Meyer, A.J.; Bangash, S.A.K.; Zheng, Z.L.; Leustek, T. Arabidopsis  $\gamma$ -Glutamylcyclotransferase Affects Glutathione Content and Root System Architecture during Sulfur Starvation. *New Phytol.* **2019**, *221*, 1387–1397. [[CrossRef](#)]
80. Dündar, E.; Bush, D.R. BAT1, a Bidirectional Amino Acid Transporter in Arabidopsis. *Planta* **2009**, *229*, 1047–1056. [[CrossRef](#)]
81. Russnak, R.; Konczal, D.; McIntire, S.L. A Family of Yeast Proteins Mediating Bidirectional Vacuolar Amino Acid Transport. *J. Biol. Chem.* **2001**, *276*, 23849–23857. [[CrossRef](#)]
82. Zhao, L.; Zhang, W.; Yang, Y.; Li, Z.; Li, N.; Qi, S.; Crawford, N.M.; Wang, Y. The Arabidopsis NLP7 Gene Regulates Nitrate Signaling via NRT1.1-Dependent Pathway in the Presence of Ammonium. *Sci. Rep.* **2018**, *8*, 1487. [[CrossRef](#)]
83. Fischer, W.; Kwart, M.; Hummel, S.; Frommer, W.B. Substrate Specificity and Expression Profile of Amino Acid Transporters (AAPs) in Arabidopsis. *J. Biol. Chem.* **1995**, *270*, 16315–16320. [[CrossRef](#)] [[PubMed](#)]
84. Planchais, S.; Cabassa, C.; Toka, I.; Justin, A.M.; Renou, J.P.; Savouré, A.; Carol, P. BASIC AMINO ACID CARRIER 2 Gene Expression Modulates Arginine and Urea Content and Stress Recovery in Arabidopsis Leaves. *Front. Plant Sci.* **2014**, *5*, 330. [[CrossRef](#)] [[PubMed](#)]
85. Pratelli, R.; Voll, L.M.; Horst, R.J.; Frommer, W.B.; Pilot, G. Stimulation of Nonselective Amino Acid Export by Glutamine Dumper Proteins. *Plant Physiol.* **2010**, *152*, 762–773. [[CrossRef](#)] [[PubMed](#)]
86. Diederichsen, A.; Kusters, P.M.; Kessler, D.; Baines, Z.; Gugel, R.K. Assembling a Core Collection from the Flax World Collection Maintained by Plant Gene Resources of Canada. *Genet. Resour. Crop. Evol.* **2013**, *60*, 1479–1485. [[CrossRef](#)]
87. Sertse, D.; You, F.M.; Ravichandran, S.; Soto-Cerda, B.J.; Duguid, S.; Cloutier, S. Loci Harboring Genes with Important Role in Drought and Related Abiotic Stress Responses in Flax Revealed by Multiple GWAS Models. *Theor. Appl. Genet.* **2021**, *134*, 191–212. [[CrossRef](#)]
88. Sertse, D.; You, F.M.; Ravichandran, S.; Cloutier, S. The Complex Genetic Architecture of Early Root and Shoot Traits in Flax Revealed by Genome-Wide Association Analyses. *Front. Plant Sci.* **2019**, *10*, 1483. [[CrossRef](#)]
89. Chen, J.; Liu, L.; Wang, Z.; Zhang, Y.; Sun, H.; Song, S.; Bai, Z.; Lu, Z.; Li, C. Nitrogen Fertilization Increases Root Growth and Coordinates the Root–Shoot Relationship in Cotton. *Front. Plant Sci.* **2020**, *11*, 880. [[CrossRef](#)]
90. Myles, S.; Peiffer, J.; Brown, P.J.; Ersoz, E.S.; Zhang, Z.; Costich, D.E.; Buckler, E. Association Mapping: Critical Considerations Shift from Genotyping to Experimental Design. *Plant Cell* **2009**, *21*, 2194–2202. [[CrossRef](#)]
91. Shi, H.; Chen, M.; Gao, L.; Wang, Y.; Bai, Y.; Yan, H.; Xu, C.; Zhou, Y.; Xu, Z.; Chen, J.; et al. Genome-Wide Association Study of Agronomic Traits Related to Nitrogen Use Efficiency in Wheat. *Theor. Appl. Genet.* **2022**, *135*, 4289–4302. [[CrossRef](#)]
92. Fu, Y.; Liu, J.; Xia, Z.; Wang, Q.; Zhang, S.; Zhang, G.; Lu, H. Genome-Wide Association Studies of Maize Seedling Root Traits under Different Nitrogen Levels. *Plants* **2022**, *11*, 1417. [[CrossRef](#)]
93. Karunarathne, S.D.; Han, Y.; Zhang, X.Q.; Zhou, G.; Hill, C.B.; Chen, K.; Angessa, T.; Li, C. Genome-Wide Association Study and Identification of Candidate Genes for Nitrogen Use Efficiency in Barley (*Hordeum vulgare* L.). *Front. Plant Sci.* **2020**, *11*, 571912. [[CrossRef](#)] [[PubMed](#)]
94. Soto-Cerda, B.J.; Cloutier, S.; Quian, R.; Gajardo, H.A.; Olivos, M.; You, F.M. Genome-Wide Association Analysis of Mucilage and Hull Content in Flax (*Linum usitatissimum* L.) Seeds. *Int. J. Mol. Sci.* **2018**, *19*, 2870. [[CrossRef](#)] [[PubMed](#)]
95. He, L.; Xiao, J.; Rashid, K.Y.; Yao, Z.; Li, P.; Jia, G.; Wang, X.; Cloutier, S.; You, F.M. Genome-Wide Association Studies for Pasm Resistance in Flax (*Linum usitatissimum* L.). *Front. Plant Sci.* **2019**, *9*, 1982. [[CrossRef](#)] [[PubMed](#)]
96. Xie, D.; Dai, Z.; Yang, Z.; Tang, Q.; Sun, J.; Yang, X.; Song, X.; Lu, Y.; Zhao, D.; Zhang, L.; et al. Genomic Variations and Association Study of Agronomic Traits in Flax. *BMC Genom.* **2018**, *19*, 512. [[CrossRef](#)]
97. You, F.M.; Xiao, J.; Li, P.; Yao, Z.; Jia, G.; He, L.; Kumar, S.; Soto-Cerda, B.; Duguid, S.D.; Booker, H.M.; et al. Genome-Wide Association Study and Selection Signatures Detect Genomic Regions Associated with Seed Yield and Oil Quality in Flax. *Int. J. Mol. Sci.* **2018**, *19*, 2303. [[CrossRef](#)]
98. Soto-Cerda, B.J.; Cloutier, S.; Gajardo, H.A.; Aravena, G.; Quian, R.; You, F.M. Drought Response of Flax Accessions and Identification of Quantitative Trait Nucleotides (QTNs) Governing Agronomic and Root Traits by Genome-Wide Association Analysis. *Mol. Breed.* **2020**, *40*, 1–24. [[CrossRef](#)]
99. Zhang, Y.M.; Jia, Z.; Dunwell, J.M. Editorial: The Applications of New Multi-Locus Gwas Methodologies in the Genetic Dissection of Complex Traits. *Front. Plant Sci.* **2019**, *10*, 100. [[CrossRef](#)]
100. Soto-Cerda, B.J.; Aravena, G.; Cloutier, S. Genetic Dissection of Flowering Time in Flax (*Linum usitatissimum* L.) through Single- and Multi-Locus Genome-Wide Association Studies. *Mol. Genet. Genom.* **2021**, *296*, 877–891. [[CrossRef](#)]
101. You, F.M.; Rashid, K.Y.; Zheng, C.; Khan, N.; Li, P.; Xiao, J.; He, L.; Yao, Z.; Cloutier, S. Insights into the Genetic Architecture and Genomic Prediction of Powdery Mildew Resistance in Flax (*Linum usitatissimum* L.). *Int. J. Mol. Sci.* **2022**, *23*, 4960. [[CrossRef](#)]
102. Fan, X.; Zhang, W.; Zhang, N.; Chen, M.; Zheng, S.; Zhao, C.; Han, J.; Liu, J.; Zhang, X.; Song, L.; et al. Identification of QTL Regions for Seedling Root Traits and Their Effect on Nitrogen Use Efficiency in Wheat (*Triticum aestivum* L.). *Theor. Appl. Genet.* **2018**, *131*, 2677–2698. [[CrossRef](#)]

103. Zhu, J.; Kaeppler, S.M.; Lynch, J.P. Mapping of QTLs for Lateral Root Branching and Length in Maize (*Zea mays* L.) under Differential Phosphorus Supply. *Theor. Appl. Genet.* **2005**, *111*, 688–695. [[CrossRef](#)] [[PubMed](#)]
104. Tiwari, J.K.; Buckseth, T.; Zinta, R.; Saraswati, A.; Singh, R.K.; Rawat, S.; Dua, V.K.; Chakrabarti, S.K. Transcriptome Analysis of Potato Shoots, Roots and Stolons under Nitrogen Stress. *Sci. Rep.* **2020**, *10*, 1152. [[CrossRef](#)] [[PubMed](#)]
105. Xin, W.; Zhang, L.; Gao, J.; Zhang, W.; Yi, J.; Zhen, X.; Bi, C.; He, D.; Liu, S.; Zhao, X. Adaptation Mechanism of Roots to Low and High Nitrogen Revealed by Proteomic Analysis. *Rice* **2021**, *14*, 5. [[CrossRef](#)] [[PubMed](#)]
106. Iqbal, A.; Dong, Q.; Wang, X.; Gui, H.; Zhang, H.; Zhang, X.; Song, M. Transcriptome Analysis Reveals Differences in Key Genes and Pathways Regulating Carbon and Nitrogen Metabolism in Cotton Genotypes under N Starvation and Resupply. *Int. J. Mol. Sci.* **2020**, *21*, 1500. [[CrossRef](#)]
107. Goel, P.; Sharma, N.K.; Bhuria, M.; Sharma, V.; Chauhan, R.; Pathania, S.; Swarnkar, M.K.; Chawla, V.; Acharya, V.; Shankar, R.; et al. Transcriptome and Co-Expression Network Analyses Identify Key Genes Regulating Nitrogen Use Efficiency in *Brassica Juncea* L. *Sci. Rep.* **2018**, *8*, 7451. [[CrossRef](#)]
108. Liu, S.H.; Shen, P.C.; Chen, C.Y.; Hsu, A.N.; Cho, Y.C.; Lai, Y.L.; Chen, F.H.; Li, C.Y.; Wang, S.C.; Chen, M.; et al. DriverDBv3: A Multi-Omics Database for Cancer Driver Gene Research. *Nucleic Acids Res.* **2020**, *48*, D863–D870. [[CrossRef](#)]
109. Wu, Y.; Shi, H.; Yu, H.; Ma, Y.; Hu, H.; Han, Z.; Zhang, Y.; Zhen, Z.; Yi, L.; Hou, J. Combined GWAS and Transcriptome Analyses Provide New Insights Into the Response Mechanisms of Sunflower Against Drought Stress. *Front. Plant Sci.* **2022**, *13*, 847435. [[CrossRef](#)]
110. He, F.; Zhang, F.; Jiang, X.; Long, R.; Wang, Z.; Chen, Y.; Li, M.; Gao, T.; Yang, T.; Wang, C.; et al. A Genome-Wide Association Study Coupled With a Transcriptomic Analysis Reveals the Genetic Loci and Candidate Genes Governing the Flowering Time in Alfalfa (*Medicago sativa* L.). *Front. Plant Sci.* **2022**, *13*, 913947. [[CrossRef](#)]
111. Wei, Z.; Yuan, Q.; Lin, H.; Li, X.; Zhang, C.; Gao, H.; Zhang, B.; He, H.; Liu, T.; Jie, Z.; et al. Linkage Analysis, GWAS, Transcriptome Analysis to Identify Candidate Genes for Rice Seedlings in Response to High Temperature Stress. *BMC Plant Biol.* **2021**, *21*, 85. [[CrossRef](#)]
112. Wong, C.K.; Bernardo, R. Genomewide Selection in Oil Palm: Increasing Selection Gain per Unit Time and Cost with Small Populations. *Theor. Appl. Genet.* **2008**, *116*, 815–824. [[CrossRef](#)]
113. Lorenzana, R.E.; Bernardo, R. Accuracy of Genotypic Value Predictions for Marker-Based Selection in Biparental Plant Populations. *Theor. Appl. Genet.* **2009**, *120*, 151–161. [[CrossRef](#)] [[PubMed](#)]
114. Hosseini-Vardanjani, S.M.; Shariati, M.M.; Shahrebabak, H.M.; Tahmoorespur, M. Incorporating Prior Knowledge of Principal Components in Genomic Prediction. *Front. Genet.* **2018**, *9*, 289. [[CrossRef](#)] [[PubMed](#)]
115. Yuan, Y.; Cairns, J.E.; Babu, R.; Gowda, M.; Makumbi, D.; Magorokosho, C.; Zhang, A.; Liu, Y.; Wang, N.; Hao, Z.F.; et al. Genome-Wide Association Mapping and Genomic Prediction Analyses Reveal the Genetic Architecture of Grain Yield and Flowering Time under Drought and Heat Stress Conditions in Maize. *Front. Plant Sci.* **2019**, *9*, 1919. [[CrossRef](#)] [[PubMed](#)]
116. Zhang-Biehn, S.; Fritz, A.K.; Zhang, G.; Evers, B.; Regan, R.; Poland, J. Accelerating Wheat Breeding for End-Use Quality through Association Mapping and Multivariate Genomic Prediction. *Plant Genome* **2021**, *14*, e20164. [[CrossRef](#)] [[PubMed](#)]
117. Muñoz-Huerta, R.F.; Guevara-Gonzalez, R.G.; Contreras-Medina, L.M.; Torres-Pacheco, I.; Prado-Olivarez, J.; Ocampo-Velazquez, R.V. A Review of Methods for Sensing the Nitrogen Status in Plants: Advantages, Disadvantages and Recent Advances. *Sensors* **2013**, *13*, 10823–10843. [[CrossRef](#)] [[PubMed](#)]
118. VSN International GenStat for Windows 2015. Available online: <https://vsni.co.uk/software/genstat> (accessed on 7 January 2023).
119. Bouslama, M.; Schapaugh, W.T. Stress Tolerance in Soybeans. I. Evaluation of Three Screening Techniques for Heat and Drought Tolerance. *Crop. Sci.* **1984**, *24*, 933–937. [[CrossRef](#)]
120. Fernandez, G.C.J. *Effective Selection Criteria for Assessing Plant Stress Tolerance*; Kuo, C.G., Ed.; International Symposium on Adaptation of Food Crops to Temperature and Water Stress: Tainan, Taiwan, 1992.
121. Wickham, H. *Ggplot2—Elegant Graphics for Data Analysis*, 2nd ed.; Springer: New York, NY, USA, 2016; ISBN 978-3-319-24277-4.
122. Pritchard, J.K.; Stephens, M.; Rosenberg, N.A.; Donnelly, P. Association Mapping in Structured Populations. *Am. J. Hum. Genet.* **2000**, *67*, 170–181. [[CrossRef](#)]
123. Evanno, G.; Regnaut, S.; Goudet, J. Detecting the Number of Clusters of Individuals Using the Software STRUCTURE: A Simulation Study. *Mol. Ecol.* **2005**, *14*, 2611–2620. [[CrossRef](#)]
124. Bradbury, P.J.; Zhang, Z.; Kroon, D.E.; Casstevens, T.M.; Ramdoss, Y.; Buckler, E.S. TASSEL: Software for Association Mapping of Complex Traits in Diverse Samples. *Bioinformatics* **2007**, *23*, 2633–2635. [[CrossRef](#)]
125. Wen, Y.J.; Zhang, H.; Ni, Y.L.; Huang, B.; Zhang, J.; Feng, J.Y.; Wang, S.B.; Dunwell, J.M.; Zhang, Y.M.; Wu, R. Methodological Implementation of Mixed Linear Models in Multi-Locus Genome-Wide Association Studies. *Brief Bioinform.* **2018**, *19*, 700–712. [[CrossRef](#)]
126. Tamba, C.L.; Zhang, Y.-M. A Fast MrMLM Algorithm for Multi-Locus Genome-Wide Association Studies. *bioRxiv* **2018**. [[CrossRef](#)]
127. Tamba, C.L.; Ni, Y.L.; Zhang, Y.M. Iterative Sure Independence Screening EM-Bayesian LASSO Algorithm for Multi-Locus Genome-Wide Association Studies. *PLoS Comput. Biol.* **2017**, *13*, e1005357. [[CrossRef](#)] [[PubMed](#)]
128. Wang, S.B.; Feng, J.Y.; Ren, W.L.; Huang, B.; Zhou, L.; Wen, Y.J.; Zhang, J.; Dunwell, J.M.; Xu, S.; Zhang, Y.M. Improving Power and Accuracy of Genome-Wide Association Studies via a Multi-Locus Mixed Linear Model Methodology. *Sci. Rep.* **2016**, *6*, 19444. [[CrossRef](#)] [[PubMed](#)]

129. Ren, W.L.; Wen, Y.J.; Dunwell, J.M.; Zhang, Y.M. PKWmEB: Integration of Kruskal-Wallis Test with Empirical Bayes under Polygenic Background Control for Multi-Locus Genome-Wide Association Study. *Heredity* **2018**, *120*, 208–218. [[CrossRef](#)] [[PubMed](#)]
130. Zhang, J.; Feng, J.Y.; Ni, Y.L.; Wen, Y.J.; Niu, Y.; Tamba, C.L.; Yue, C.; Song, Q.; Zhang, Y.M. PLARmEB: Integration of Least Angle Regression with Empirical Bayes for Multilocus Genome-Wide Association Studies. *Heredity* **2017**, *118*, 517–524. [[CrossRef](#)]
131. Zhang, Y.W.; Tamba, C.L.; Wen, Y.J.; Li, P.; Ren, W.L.; Ni, Y.L.; Gao, J.; Zhang, Y.M. MrMLM v4.0.2: An R Platform for Multi-Locus Genome-Wide Association Studies. *Genom. Proteom. Bioinform.* **2020**, *18*, 481–487. [[CrossRef](#)]
132. Vos, P.G.; Paulo, M.J.; Voorrips, R.E.; Visser, R.G.F.; van Eck, H.J.; van Eeuwijk, F.A. Evaluation of LD Decay and Various LD-Decay Estimators in Simulated and SNP-Array Data of Tetraploid Potato. *Theor. Appl. Genet.* **2017**, *130*, 123–135. [[CrossRef](#)]
133. Bolger, A.M.; Lohse, M.; Usadel, B. Trimmomatic: A Flexible Trimmer for Illumina Sequence Data. *Bioinformatics* **2014**, *30*, 2114–2120. [[CrossRef](#)]
134. Kim, D.; Paggi, J.M.; Park, C.; Bennett, C.; Salzberg, S.L. Graph-Based Genome Alignment and Genotyping with HISAT2 and HISAT-Genotype. *Nat. Biotechnol.* **2019**, *37*, 907–915. [[CrossRef](#)]
135. Li, H.; Handsaker, B.; Wysoker, A.; Fennell, T.; Ruan, J.; Homer, N.; Marth, G.; Abecasis, G.; Durbin, R. The Sequence Alignment/Map Format and SAMtools. *Bioinformatics* **2009**, *25*, 2078–2079. [[CrossRef](#)]
136. Liao, Y.; Smyth, G.K.; Shi, W. FeatureCounts: An Efficient General Purpose Program for Assigning Sequence Reads to Genomic Features. *Bioinformatics* **2014**, *30*, 923–930. [[CrossRef](#)] [[PubMed](#)]
137. Love, M.I.; Huber, W.; Anders, S. Moderated Estimation of Fold Change and Dispersion for RNA-Seq Data with DESeq2. *Genome Biol.* **2014**, *15*, 550. [[CrossRef](#)] [[PubMed](#)]
138. Aramaki, T.; Blanc-Mathieu, R.; Endo, H.; Ohkubo, K.; Kanehisa, M.; Goto, S.; Ogata, H. KofamKOALA: KEGG Ortholog Assignment Based on Profile HMM and Adaptive Score Threshold. *Bioinformatics* **2020**, *36*, 2251–2252. [[CrossRef](#)] [[PubMed](#)]
139. Fernandes, S.B.; Dias, K.O.G.; Ferreira, D.F.; Brown, P.J. Efficiency of Multi-Trait, Indirect, and Trait-Assisted Genomic Selection for Improvement of Biomass Sorghum. *Theor. Appl. Genet.* **2018**, *131*, 747–755. [[CrossRef](#)]
140. Pérez, P.; De Los Campos, G. Genome-Wide Regression and Prediction with the BGLR Statistical Package. *Genetics* **2014**, *198*, 483–495. [[CrossRef](#)]
141. De Los Campos, G.; Pérez, P.; Vazquez, A.I.; Crossa, J. Genome-Enabled Prediction Using the BLR (Bayesian Linear Regression) R-Package. *Methods Mol. Biol.* **2013**, *1019*, 299–320. [[CrossRef](#)]

**Disclaimer/Publisher’s Note:** The statements, opinions and data contained in all publications are solely those of the individual author(s) and contributor(s) and not of MDPI and/or the editor(s). MDPI and/or the editor(s) disclaim responsibility for any injury to people or property resulting from any ideas, methods, instructions or products referred to in the content.